We are IntechOpen, the world's leading publisher of Open Access books Built by scientists, for scientists

6,900
Open access books available

185,000
International authors and editors

200M
Downloads

Our authors are among the

154
Countries delivered to

TOP 1%
most cited scientists

12.2%
Contributors from top 500 universities



WEB OF SCIENCE™

Selection of our books indexed in the Book Citation Index in Web of Science™ Core Collection (BKCI)

Interested in publishing with us?
Contact book.department@intechopen.com

Numbers displayed above are based on latest data collected.
For more information visit www.intechopen.com



Chapter 2

Random Beamforming in Multi – User MIMO Systems

Hieu Duy Nguyen, Rui Zhang and Hon Tat Hui

Additional information is available at the end of the chapter

http://dx.doi.org/10.5772/57131

1. Introduction

Wireless communication paradigm has evolved from single-user single-input single-output (SISO) and multiple-input multiple-output (MIMO) systems to multi-user (MU) MIMO counterparts, which are shown greatly improving the rate performance by transmitting to multiple users simultaneously. The sum-capacity and the capacity region of a single-cell MU MIMO downlink system or the so-called MIMO broadcast channel (MIMO-BC) can be attained by the nonlinear "Dirty Paper Coding (DPC)" scheme [1] [2] [3]. However, DPC requires a high implementation complexity due to the non-linear successive encoding/decoding at the transmitter/receiver, and is thus not suitable for real-time applications. Other studies have proposed to use alternative linear precoding schemes for the MIMO-BC, e.g., the block-diagonalization scheme [4], to reduce the complexity. More information on the key developments of single-cell MIMO communication can be found in, for example, [5] [6] [7].

The performance of a multi-cell MIMO-BC setup, however, is not well understood. It is worth noting that the multi-cell downlink system can be modelled in general as an interference channel (IC) setup. Characterization of the capacity region of the Gaussian IC is still an open problem even for the two-user case [8]. An important development recently is the so-called "interference alignment (IA)" transmission scheme (see, e.g., [9] and references therein). With the aid of IA, the maximum achievable degrees of freedom (DoF), in which the DoF is defined as the sum-rate normalized by the logarithm of the signal-to-noise ratio (SNR) as the SNR goes to infinity or the so-called "pre-log" factor, has been obtained for various ICs to provide useful insights on designing the optimal transmission for interference-limited MU systems. Besides IA-based studies for the high-SNR regime, there is a vast body of works in the literature which investigated the multi-cell cooperative downlink precoding/beamforming at a given finite user's SNR. These works are typically categorized based on two different assumptions on the cooperation level of base stations (BSs). For the case of "fully cooperative" multi-cell systems with global

INTECH
open science | open minds

© 2013 Nguyen et al.; licensee InTech. This is a paper distributed under the terms of the Creative Commons Attribution License (http://creativecommons.org/licenses/by/3.0), which permits unrestricted use, distribution, and reproduction in any medium, provided the original work is properly cited.

transmit message sharing across all the BSs, a virtual MIMO-BC channel is equivalently formed. Therefore, existing single-cell downlink precoding techniques can be applied (see, e.g., [10] [11] [12] and references therein) with a non-trivial modification to deal with the per-BS power constraints as compared to the conventional sum-power constraint for the single-cell MIMO-BC case. In contrast, if transmit messages are only locally known at each BS, coordinated precoding/beamforming can be implemented among BSs to control the inter-cell interference (ICI) to their best effort [13] [14]. In [15] [16] [17], various parametrical characterizations of the Pareto boundary of the achievable rate region have been obtained for the multiple-input single-output (MISO) IC with coordinated transmit beamforming and single-user detection.

More important, most of the proposed precoding schemes, in single- or multi-cell case, rely on the assumption of perfect channel state information (CSI) for all the intra- and inter-cell links at the transmitter, which may not be realistic in practical cellular systems with a large number of users. Consequently, the study of quantized channel feedback for the MIMO BC has been recently a very active area of research (see, e.g., [18] and references therein).

The single-beam "opportunistic beamforming (OBF)" and multi-beam "random beamforming (RBF)" schemes for the single-cell MISO-BC, introduced in [19] and [20], respectively, therefore attract a lot of attention since they require only *partial* CSI feedback to the BS. The fundamental idea is to exploit the multi-user diversity gain, by employing *opportunistic user scheduling*, to combat the inter-beam interferences. The achievable sum-rate with RBF in a single-cell system has been shown to scale identically to that with the optimal DPC scheme assuming perfect CSI as the number of users goes to infinity, for any given user's signal-to-noise ratio (SNR) [20] [21]. Essentially, the result implies that the intra-cell interference in a single-cell RBF system can be completely eliminated when the number of users are sufficiently large, and an "interference-free" MU broadcast system is attainable. This thus shows the optimality of the single-cell RBF and motives other studies on opportunistic communication.

Although substantial subsequent investigations and/or extensions of the single-cell RBF have been pursued, there are very few works on the performance of the RBF scheme in a more realistic multi-cell setup, where the ICI becomes a dominant factor. It is worth noting that as the universal frequency reuse becomes more favourable in future generation cellular systems, ICI becomes a more serious issue as compared to the traditional case with only a fractional frequency reuse.

One objective of this chapter is to present a literature survey on the vast body of works studying the single-cell OBF/RBF. The main purpose, however, is to introduce the recent investigations on multi-cell RBF systems. In this chapter, we first review the achievable rates of multi-cell RBF in finite-SNR regime. Such results, albeit important, do not provide any insight to the impact of the interferences on the system throughput. This motivates us to introduce the high-SNR/DoF analysis proposed in [22] and [23], which is useful in characterizing the performance of RBF under multi-user diversity and interference effects. Furthermore, it provides new insights on the role of *spatial receive diversity* in RBF, which is not well understood so far. It is revealed that receive diversity is significantly beneficial to the rate performance of multi-cell RBF systems [24]. This conclusion, interestingly, sharply contrasts with one based on the traditional asymptotic analysis, i.e., assuming that the number of users goes to infinity for any given user's SNR.

http://dx.doi.org/10.5772/57131

The remainder of this chapter is organized as follows. Section 2 describes the multi-cell MIMO-BC system model and the MISO/MIMO RBF schemes. Section 3 presents a literature survey on the single-cell OBF/RBF. Section 4 investigates the multi-cell RBF under finite-SNR regime. The high-SNR/DoF analysis is introduced in Section 5, based on which we study the interplay between the multi-user diversity, spatial receive diversity and spatial multiplexing gains achievable in RBF. Finally, Section 6 ends the chapter with some concluding remarks.

Notations: Scalars, vectors, and matrices are denoted by lower-case, bold-face lower-case, and bold-face higher-case letters, respectively. The transpose and conjugate transpose operators are denoted as $(\cdot)^T$ and $(\cdot)^H$, respectively. $\mathbb{E}[\cdot]$ denotes the statistical expectation. $\mathbf{Tr}(\cdot)$ represents the trace of a matrix. The distribution of a circularly symmetric complex Gaussian random variable with zero mean and covariance σ^2 is denoted by $\mathcal{CN}(0,\sigma^2)$; and $\sim$ stands for "distributed as". $\mathbb{C}^{x\times y}$ denotes the space of $x \times y$ complex matrices.

2. System model

This section introduces the multi-cell system model and RBF schemes used throughout this chapter. Particularly, we consider a C-cell MIMO-BC system with K_c mobile stations (MSs) in the c-th cell, $c = 1, \cdots, C$. For the ease of analysis, we assume that all BSs/MSs have the same number of transmit/receive antennas, denoted as N_T and N_R, respectively. We also assume a "homogeneous" channel setup, in which the signal and ICI powers between users of one cell are identical. At each communication time, the c-th BS transmits $M_c \leq N_T$ orthonormal beams with M_c antennas and selects M_c from K_c users for transmission. Suppose that the channels are flat-fading and constant over each transmission period of interest. The received signal of user k in the c-th cell is

$$\boldsymbol{y}_k^{(c)} = \boldsymbol{H}_k^{(c,c)} \sum_{m=1}^{M_c} \boldsymbol{\phi}_m^{(c)} s_m^{(c)} + \sum_{l=1,\, l\neq c}^{C} \sqrt{\gamma_{l,c}} \boldsymbol{H}_k^{(l,c)} \sum_{m=1}^{M_l} \boldsymbol{\phi}_m^{(l)} s_m^{(l)} + \boldsymbol{z}_k^{(c)}, \tag{1}$$

where $\boldsymbol{H}_k^{(l,c)} \in \mathbb{C}^{N_R \times M_l}$ denotes the channel matrix between the l-th BS and the k-th user of the c-th cell, which consists of independent and identically distributed (i.i.d.) $\sim \mathcal{CN}(0,1)$ elements; $\boldsymbol{\phi}_m^{(c)} \in \mathbb{C}^{M_c \times 1}$ and $s_m^{(c)}$ are the m-th randomly generated beamforming vector of unit norm and transmitted data symbol from the c-th BS, respectively; it is assumed that each BS has the total sum power, P_T, i.e., $\mathbf{Tr}\left(\mathbb{E}[\boldsymbol{s_c}\boldsymbol{s_c^H}]\right) \leq P_T$, where $\boldsymbol{s}_c = [s_1^{(c)}, \cdots, s_{M_c}^{(c)}]^T$; $\gamma_{l,c} < 1$ stands for the signal attenuation from the l-th BS to any user of the c-th cell, $l \neq c$; and $\boldsymbol{z}_k^{(c)} \in \mathbb{C}^{N_R \times 1}$ is the additive white Gaussian noise (AWGN) vector, of which each element is $\sim \mathcal{CN}(0,\sigma^2)$, $\forall k, c$. In the c-th cell, the total SNR, the SNR per beam, and the interference-to-noise ratio (INR) per beam from the l-th cell, $l \neq c$, are denoted as $\rho = P_T/\sigma^2$, $\eta_c = P_T/(M_c\sigma^2)$, and $\mu_{l,c} = \gamma_{l,c}P_T/(M_l\sigma^2)$, respectively.

2.1. Multi-cell MISO RBF

In this case, $N_R = 1$ and the system model in (1) reduces to

$$y_k^{(c)} = \boldsymbol{h}_k^{(c,c)} \sum_{m=1}^{M_c} \boldsymbol{\phi}_m^{(c)} s_m^{(c)} + \sum_{l=1,\, l\neq c}^{C} \sqrt{\gamma_{l,c}} \boldsymbol{h}_k^{(l,c)} \sum_{m=1}^{M_l} \boldsymbol{\phi}_m^{(l)} s_m^{(l)} + z_k^{(c)}, \tag{2}$$

We consider a multi-cell RBF scheme, in which all BSs in different cells are assumed to be able to implement the conventional single-cell RBF [20] in a time synchronized manner, which is described as follows:

- In the training phase, the c-th BS generates M_c orthonormal beams, $\boldsymbol{\phi}_1^{(c)}, \cdots, \boldsymbol{\phi}_{M_c}^{(c)}$, and uses them to broadcast the training signals to all users in the c-th cell. The total power of each BS is assumed to be distributed equally over M_c beams.
- Feedback scheme: Each user in the c-th cell measures the signal-to-interference-plus-noise ratio (SINR) value for each of M_c beams (shown in (3) below), and feeds this scalar value together with the corresponding beam index back to the BS.

$$\begin{aligned} \mathrm{SINR}_{k,m}^{(c)} &= \frac{\frac{P_T}{M_c} \left| \boldsymbol{h}_k^{(c,c)} \boldsymbol{\phi}_m^{(c)} \right|^2}{\sigma^2 + \frac{P_T}{M_c} \sum_{i=1, i\neq m}^{M_c} \left| \boldsymbol{h}_k^{(c,c)} \boldsymbol{\phi}_i^{(c)} \right|^2 + \sum_{l=1, l\neq c}^{C} \gamma_{l,c} \frac{P_T}{M_l} \sum_{i=1}^{M_l} \left| \boldsymbol{h}_k^{(l,c)} \boldsymbol{\phi}_i^{(l)} \right|^2} \\ &= \frac{\eta_c \left| \boldsymbol{h}_k^{(c,c)} \boldsymbol{\phi}_m^{(c)} \right|^2}{1 + \eta_c \sum_{i=1, i\neq m}^{M_c} \left| \boldsymbol{h}_k^{(c,c)} \boldsymbol{\phi}_i^{(c)} \right|^2 + \sum_{l=1, l\neq c}^{C} \mu_{l,c} \sum_{i=1}^{M_l} \left| \boldsymbol{h}_k^{(l,c)} \boldsymbol{\phi}_i^{(l)} \right|^2}, \end{aligned} \tag{3}$$

  where $m = 1, \cdots, M_c$.
- Opportunistic scheduling: The c-th BS schedules transmission to a set of M_c users for each time by assignning its m-th beam to the user with the highest SINR, i.e.,

$$k_m^{(c)} = \arg \max_{k \in \{1, \cdots, K_c\}} \mathrm{SINR}_{k,m}^{(c)}. \tag{4}$$

Then, the achievable average sum-rate in bits-per-second-per-Hz (bps/Hz) of the c-th cell is given by

$$R_{\mathrm{RBF}}^{(c)} = \mathbb{E}\left[\sum_{m=1}^{M_c} \log_2 \left(1 + \mathrm{SINR}_{k_m^{(c)},m}^{(c)} \right) \right] = M_c \mathbb{E}\left[\log_2 \left(1 + \mathrm{SINR}_{k_1^{(c)},1}^{(c)} \right) \right]. \tag{5}$$

Note that a different feedback scheme for single-cell RBF systems is considered in [20]. Sharif *et. al.* assumes that each user can only sends its maximum SINR, i.e., $\max_{1\leq m\leq M} \mathrm{SINR}_{k,m}$, along with the index m in which the SINR is maximized. The objective for introducing this scheme is to get a fair comparison with OBF. In this case, (5) is only a close approximation of the c-th sum rate by ignoring the small probability that one user may be assigned more than one beams for transmission and diminishes to zero as $K_c \to \infty$ [20]. In this chapter, the modified feedback scheme is considered since the focus is the rate performance under multi-user diversity, spatial receive diversity, and interference-limited effects.

http://dx.doi.org/10.5772/57131

2.2. Multi-cell MIMO RBF schemes

With multiple antennas, the MSs can apply receive diversity techniques to enhance the performance. In this chapter, we consider the three receiver designs, i.e., minimum-mean-square-error (MMSE), match-filter (MF), and antenna selection (AS), respectively. The necessity of employing such suboptimal schemes arises when MSs are constrained by the time-delay criterion or the complexity of the MMSE receiver. We formally define the multi-cell RBF with MMSE, MF, and AS receiver, denoted as RBF-MMSE, RBF-MF, and RBF-AS, respectively, as follows:

1. Training phase:
   a) The c-th BS generates M_c orthonormal beams, $\boldsymbol{\phi}_1^{(c)}, \cdots, \boldsymbol{\phi}_{M_c}^{(c)}$, and uses them to broadcast the training signals to all users in all cells. The total power of the c-th BS is assumed to be distributed equally over M_c beams.
   b1) MMSE: For the m-th beam, user k in the c-th cell does the following steps:
      i. Estimate the effective channel through training with the c-th BS: $\sqrt{\frac{P_T}{M_c}}\tilde{\boldsymbol{h}}_{k,m}^{(c,c)} = \sqrt{\frac{P_T}{M_c}}\boldsymbol{H}_k^{(c,c)}\boldsymbol{\phi}_m^{(c)}$.
      ii. Estimate the interference-plus-noise covariance matrix through training with all BSs:

$$\boldsymbol{W}_k^{(c)} = \frac{P_T}{M_c}\tilde{\boldsymbol{H}}_{k,-m}^{(c,c)}\left(\tilde{\boldsymbol{H}}_{k,-m}^{(c,c)}\right)^H + \sum_{l=1,l\neq c}^{C}\frac{P_T\gamma_{l,c}}{M_l}\tilde{\boldsymbol{H}}_k^{(l,c)}\left(\tilde{\boldsymbol{H}}_k^{(l,c)}\right)^H + \sigma^2\boldsymbol{I}, \tag{6}$$

      in which $\tilde{\boldsymbol{H}}_{k,-m}^{(c,c)} = \boldsymbol{H}_k^{(c,c)}\,[\boldsymbol{\phi}_1^{(c)}, \cdots, \boldsymbol{\phi}_{m-1}^{(c)}, \boldsymbol{\phi}_{m+1}^{(c)}, \cdots, \boldsymbol{\phi}_{M_c}^{(c)}]$, and $\tilde{\boldsymbol{H}}_k^{(l,c)} = \boldsymbol{H}_k^{(c,c)}\,[\boldsymbol{\phi}_1^{(l)}, \cdots, \boldsymbol{\phi}_{M_l}^{(l)}]$.
      iii. Apply the MMSE receive beamformer, i.e., $\boldsymbol{t}_{k,m}^{(c)} = \sqrt{\frac{P_T}{M_c}}\left(\boldsymbol{W}_k^{(c)}\right)^{-1}\tilde{\boldsymbol{h}}_{k,m}^{(c,c)}$, then calculate and feedback the SINR corresponding to the m-th transmit beam $\boldsymbol{\phi}_m^{(c)}$ to the BS

$$\mathrm{SINR}_{k,m}^{(\mathrm{MMSE},c)} = \frac{P_T}{M_c}\left(\tilde{\boldsymbol{h}}_{k,m}^{(c,c)}\right)^H\left(\boldsymbol{W}_k^{(c)}\right)^{-1}\tilde{\boldsymbol{h}}_{k,m}^{(c,c)}. \tag{7}$$

   b2) MF: For the m-th beam, user k in the c-th cell does the following steps:
      i. Estimate the effective channel through training with the c-th BS: $\sqrt{\frac{P_T}{M_c}}\tilde{\boldsymbol{h}}_{k,m}^{(c,c)} = \sqrt{\frac{P_T}{M_c}}\boldsymbol{H}_k^{(c,c)}\boldsymbol{\phi}_m^{(c)}$.
      ii. Apply the MF, i.e., $\boldsymbol{t}_{k,m}^{(c)} = \tilde{\boldsymbol{h}}_{k,m}^{(c,c)} \,/\, ||\tilde{\boldsymbol{h}}_{k,m}^{(c,c)}||$. The rationale is to maximize the power received from the desired beam. The receive signal now is

$$r_{k,m}^{(c)} = \left(\boldsymbol{t}_{k,m}^{(c)}\right)^H \boldsymbol{y}_k^{(c)} = \sqrt{\frac{P_T}{M_c}} \left(\boldsymbol{t}_{k,m}^{(c)}\right)^H \tilde{\boldsymbol{h}}_{k,m}^{(c,c)} s_m^{(c)} + \sqrt{\frac{P_T}{M_c}} \left(\boldsymbol{t}_{k,m}^{(c)}\right)^H \tilde{\boldsymbol{H}}_{k,-m}^{(c,c)} \boldsymbol{s}_{-m}^{(c)} + \sum_{l=1, l\neq c} \sqrt{\frac{P_T \gamma_{l,c}}{M_l}} \left(\boldsymbol{t}_{k,m}^{(c)}\right)^H \tilde{\boldsymbol{H}}_k^{(l,c)} \boldsymbol{s}_{(l)} + \left(\boldsymbol{t}_{k,m}^{(c)}\right)^H \boldsymbol{z}_k^{(c)}, \quad (8)$$

where $s_{-m}^{(c)} = [\boldsymbol{s}_1^{(c)}, \cdots, \boldsymbol{s}_{m-1}^{(c)}, \boldsymbol{s}_{m+1}^{(c)}, \cdots, \boldsymbol{s}_{M_c}^{(c)}]$ and $s_m^{(l)} = [\boldsymbol{s}_1^{(l)}, \cdots, \boldsymbol{s}_{M_l}^{(c)}]$. Through training with all BSs, user k in the c-th cell estimates the interferences' power in (8), which can be expressed equivalently as $\left(\tilde{\boldsymbol{h}}_{k,m}^{(c,c)}\right)^H \left(\boldsymbol{W}_k^{(c)}\right) \tilde{\boldsymbol{h}}_{k,m}^{(c,c)}$, in which $\boldsymbol{W}_k^{(c)}$ is defined as in (6). Each user then calculates and feedbacks the SINR corresponding to the m-th transmit beam $\boldsymbol{\phi}_m^{(c)}$ to the BS, which can be expressed equivalently as follows

$$\mathrm{SINR}_{k,m}^{(\mathrm{MF},c)} = \frac{\frac{P_T}{M_c} ||\tilde{\boldsymbol{h}}_{k,m}^{(c,c)}||^4}{\left(\tilde{\boldsymbol{h}}_{k,m}^{(c,c)}\right)^H \left(\boldsymbol{W}_k^{(c)}\right) \tilde{\boldsymbol{h}}_{k,m}^{(c,c)}}, \quad (9)$$

Note that the k-th user in the c-th cell knows $\left(\tilde{\boldsymbol{h}}_{k,m}^{(c,c)}\right)^H \left(\boldsymbol{W}_k^{(c)}\right) \tilde{\boldsymbol{h}}_{k,m}^{(c,c)}$ but not $\boldsymbol{W}_k^{(c)}$.

b3) AS: The received signal at the n-th receive antenna of user k in the c-th cell is:

$$y_{k,n}^{(c)} = \boldsymbol{h}_{k,n}^{(c,c)} \sum_{m=1}^{M_c} \boldsymbol{\phi}_m^{(c)} s_m^{(c)} + \sum_{l=1,\ l\neq c}^{C} \sqrt{\gamma_{l,c}} \boldsymbol{h}_{k,n}^{(l,c)} \sum_{m=1}^{M_l} \boldsymbol{\phi}_m^{(l)} s_m^{(l)} + z_{k,n}^{(c)}, \quad (10)$$

where $y_{k,n}^{(c)}$ and $z_{k,n}^{(c)}$ are the n-th element of $\boldsymbol{y}_k^{(c)}$ and $\boldsymbol{z}_k^{(c)}$, respectively, and $\boldsymbol{h}_{k,n}^{(l,c)} \in \mathbb{C}^{1\times M_l}$ is the n-th row of $\boldsymbol{H}_k^{(l,c)}$, $n \in \{1, \ldots, N_R\}$, $l, c \in \{1, \ldots, C\}$. For the m-th beam and n-th antenna, user k estimates the received power of the signal and the interferences through training with the c-th BS and all BSs, respectively. The following SINR value is then calculated:

$$\mathrm{SINR}_{k,n,m}^{(\mathrm{AS},c)} = \frac{\frac{P_T}{M_c} \left|\boldsymbol{h}_{k,n}^{(c,c)} \boldsymbol{\phi}_m^{(c)}\right|^2}{\sigma^2 + \frac{P_T}{M_c} \sum_{i=1, i\neq m}^{M_c} \left|\boldsymbol{h}_{k,n}^{(c,c)} \boldsymbol{\phi}_i^{(c)}\right|^2 + \sum_{l=1, l\neq c}^{C} \gamma_{l,c} \frac{P_T}{M_l} \sum_{i=1}^{M_l} \left|\boldsymbol{h}_{k,n}^{(l,c)} \boldsymbol{\phi}_i^{(l)}\right|^2}. \quad (11)$$

Denote

$$\mathrm{SINR}_{k,m}^{(\mathrm{AS},c)} := \max_{n\in\{1,\cdots,N_R\}} \mathrm{SINR}_{k,n,m}^{(\mathrm{AS},c)}. \quad (12)$$

http://dx.doi.org/10.5772/57131

For each m-th beam, the k-th user selects antenna $n_{k,m}^{(c)}$, which corresponds to $\mathrm{SINR}_{k,m}^{(\mathrm{AS},c)}$, and feeds $\mathrm{SINR}_{k,m}^{(\mathrm{AS},c)}$ back to the BS.

2. Scheduling phase: The c-th BS assigns the m-th beam to the user with the highest SINR

$$k_m^{(\mathrm{Rx},c)} = \arg \max_{k \in \{1,\cdots,K_c\}} \mathrm{SINR}_{k,m}^{(\mathrm{Rx},c)}, \tag{13}$$

in which "Rx" denotes either MMSE, MF, or AS.

3. Transmitting phase: The c-th BS uses the m-th beam to transmit data to user $k_m^{(\mathrm{Rx},c)}$.

The achievable sum-rate in bits per second per Hz (bps/Hz) of the c-th RBF-Rx cell can be expressed as

$$R_{\text{RBF-Rx}}^{(c)} = \mathbb{E}\left[\sum_{m=1}^{M_c} \log_2\left(1 + \mathrm{SINR}_{k_m^{(\mathrm{Rx},c)},m}^{(\mathrm{Rx},c)}\right)\right] = M_c \mathbb{E}\left[\log_2\left(1 + \mathrm{SINR}_{k_1^{(\mathrm{Rx},c)},1}^{(\mathrm{Rx},c)}\right)\right]. \tag{14}$$

Remark 2.1. *The RBF-AS scheme consists of two selection processes: antenna selection at the MSs each with N_R antennas and opportunistic scheduling at the BSs with K_c's users. The rate performance of RBF-AS is therefore equal to that of the (MISO-BC) RBF with $N_R K_c$ single-antenna users in the c-th cell. The RBF-AS scheme is introduced here to provide a complete study and rigorous comparison.*

3. Literature survey on single-cell OBF/RBF

Since its introduction in the landmark paper [19], opportunistic communication has developed to a broad area with various constituent topics. In this section, we aim to present a succinct overview on the key developments of OBF/RBF, summarizing some of the most important results contributed to the field. Note that in the literature, virtually all the works consider the single-cell case. It is only quite recent that the rate performance of the multi-cell RBF and ad-hoc IC with user scheduling is explored in [24] [22] [23]. We therefore limit our survey to the single-cell OBF/RBF. In this section, the channel model (2) has $C = 1$ and the cell index c is dropped for brevity. (3) and (5) hence reduce to

$$\mathrm{SINR}_{k,m} = \frac{\frac{P_T}{M}|\boldsymbol{h}_k \boldsymbol{\phi}_m|^2}{\sigma^2 + \frac{P_T}{M}\sum_{i=1,i\neq m}^{M}|\boldsymbol{h}_k \boldsymbol{\phi}_i|^2}. \tag{15}$$

$$R_{\mathrm{RBF}} = M\mathbb{E}\left\{\log_2\left(1 + \max_{k \in \{1,\cdots,K\}} \mathrm{SINR}_{k,1}\right)\right\}. \tag{16}$$

The probability density function (PDF) and cumulative density function (CDF) of $S := \mathrm{SINR}_{k,m}, \forall k, m$ can be expressed as [20]

$$f_S(s) = \frac{e^{-s/\eta}}{(s+1)^M}\left(M - 1 + \frac{s+1}{\eta}\right). \tag{17}$$

$$F_S(s) = 1 - \frac{e^{-s/\eta}}{(s+1)^{M-1}}. \tag{18}$$

where $\eta = P_T/(M\sigma^2)$ is the SNR per beam.

3.1. Achievable rate

With the feedback scheme stated in Section 2.1, the closed-form expression for the sum rate R_{RBF} is given in the following lemma.

Lemma 3.1. *([22, Lemma 3.1], see also [55]) The average sum rate of the single-cell RBF is given by*

$$R_{RBF} = \frac{M}{\log 2}\sum_{n=1}^{K}(-1)^n\binom{K}{n}\left[\left(-\frac{n}{\eta}\right)^{n(M-1)}\frac{e^{n/\eta}Ei(-n/\eta)}{(n(M-1))!} - \sum_{m=1}^{n(M-1)}\left(-\frac{n}{\eta}\right)^{m-1}\frac{(n(M-1)-m)!}{(n(M-1))!}\right], \tag{19}$$

where $Ei(x) = \int_{-\infty}^{x}\frac{e^t}{t}dt$ is the exponential integral function.

Assuming the feedback scheme in [20], (19) becomes a close approximation of the exact sum rate, especially when the number of users K is large. The exact expression of the sum rate is derived in [25], which involves a numerical integral with the SINR CDF of the first beam:

Lemma 3.2. *([25]) Assuming the feedback scheme in [20], the average sum rate of the single-cell RBF is given by*

$$R'_{RBF} = M\int_0^{\infty}\log_2(1+x)f'_{SINR_{k_1,1}}(x)dx, \tag{20}$$

in which

$$f'_{SINR_{k_1,1}}(x) = \sum_{k=1}^{K}\frac{1}{M}\left(1-\frac{1}{M}\right)^{k-1}\frac{K!}{(K-k)!(k-1)!}\left(F_1(x)\right)^{K-k}\left[1-F_1(x)\right]^{k-1}f_1(x) + \left(1-\frac{1}{M}\right)^{K}\frac{1}{M-1}\sum_{m=2}^{M}f_{2,m}(x), \tag{21}$$

$$F_1(x) = \int_0^x f_1(t)dt, \tag{22}$$

$$f_1(x) = \sum_{m=0}^{}M-1\frac{(-1)^m M!}{(M-m-1)!m!}\exp\left(-\frac{(1+m)x}{\eta(mx-1)}\right)\times \times\frac{(M+1/\eta-1+(1/\eta-mM+m)x)(1-mx)^{M-3}}{(1+x)^M}, \tag{23}$$

$$f_{2,m}(x) = \int_0^{\infty} \int_0^{\frac{(M-m)w}{m-1}} \left(\frac{1}{\eta} + z + w\right) f_{w_m,\beta_{m:M},z_m}\left(w, x\left(\frac{1}{\rho} + z + w\right), z\right) dzdw. \quad (24)$$

Finally, the function $f_{w_m,\beta_{m:M},z_m}(w,\beta,z)$ is given in [26, (28)]

$$f_{w_m,\beta_{m:M},z_m}(w,\beta,z) = \frac{M![w-(m-1)\beta]^{m-1}}{(L-1)!(l-1)!\bar{\beta}^M} \frac{\exp\left(-\frac{w+\beta+z}{\bar{\beta}}\right)}{(m-2)!(M-m-1)!} \mathcal{U}(1-(m-1)\beta) \times \times \sum_{i=0}^{M-m} \binom{M-m}{i} (-1)^i (z-i\beta)^{M-m-1} \mathcal{U}(z-i\beta),$$
$$\beta > 0, w > (m-1)\beta, z < (M-1)\beta, \quad (25)$$

where $\mathcal{U}(x)$ is the unit step function and $\bar{\beta} = 1$ due to the Rayleigh fading channel model.

In addition, loose approximations for (5) are presented in [27] and [28]. We note that (19) involves only the exponential integral function, which is more efficiently computable than the Gaussian hyper-geometric functions in [27] [28] and the (exact) expression in Lemma 3.2. However, the sum-rate approximations in [27] and [28] can directly lead to some asymptotic results, e.g., the sum-rate scaling law $M \log_2 \log K$ as $K \to \infty$, while (19) and (20) do not.

3.2. Asymptotic analysis

The accurate expression for the achievable sum rate, albeit important, is too complicated. To reveal more insights on the performance of single-cell RBF, asymptotic analyses have been considered in other studies. There are two main approaches, namely, large-number-of-users and large-system analyses.

3.2.1. Large number of users

The conventional asymptotic investigation of OBF/RBF is to consider the number of users approaches infinity for a given finite SNR. Based on *extreme value theory* [29], one of the most important results in opportunistic communication is proved in [20][1].

Theorem 3.1. *([20, Theorem 1]) For fixed $M \leq N_T$ and P_T, the single-cell RBF sum rate grows double-logarithmically with respect to the number of users, i.e.,*

$$\lim_{K\to\infty} \frac{R_{RBF}}{M \log_2 \log K} = 1. \quad (26)$$

In [21], Sharif *et. al.* show that $N_T \log_2 \log K$ is also the rate scaling law of the optimal DPC scheme assuming perfect CSI as the number of users goes to infinity, for any given

[1] Strictly speaking, Theorem 3.1 only states for the single-cell RBF with the original feedback scheme in [20]. However, it is easy to see that the same result applies when the modified feedback scheme in Section 2.1 is considered.

user's SNR. Essentially, the result implies that the intra-cell interference in a single-cell RBF system can be completely eliminated when the number of users is sufficiently large, and an "interference-free" MU broadcast system is attainable. This important result therefore establishes the optimality of single-cell RBF and motivates further studies on opportunistic communication. Various MIMO-BC transmission schemes with different assumptions on the fading model, feedback scheme, user scheduling, etc., can be shown achieving $N_T \log_2 \log K$ as $K \to \infty$, suggesting that it is a very universal rate scaling law (see, e.g., [30] [31] [28] [32] [33] [34]). Finally, it is worth noting that the RBF sum rate grows only *logarithmically* with K, i.e., $R_{RBF} \Big/ \frac{M}{M-1} \log_2 K \to 1$ as $K \to \infty$, when the background noise is ignored [30] [33]. More discussions on the large-number-of-users analysis will be given in Section 4.1.2 and 4.2.

3.2.2. Large system

The large-system analysis is a well-known and widely-accepted method to investigate the performance of communication systems. A recent application to single-cell RBF is introduced in [35], in which a general MIMO-BC setup with MMSE receiver and different fading models is considered. Assuming the numbers of transmit/receive antennas and data beams to approach infinity at the same time with fixed ratios for any given finite SNR, Couillet *et. al.* obtain "almost closed-form" numerical solutions which provide deterministic approximations for various performance criteria. Note that although these results are derived under the large-system assumption, Monte-Carlo simulations demonstrate that they can be applied to study small-dimensional systems with modest errors. However, [35] does not consider opportunistic scheduling, which is one of the main features of RBF.

3.3. Reduced and quantized feedback in OBF/RBF

In practical systems, only a limited number of bits representing the quantized channel gain/SINR can be sent from each user to the corresponding BS. Note that the feedback schemes in Section 2.1 and [20] require the transmission of $2MK$ and $2K$ scalar values from K users, respectively, i.e., a linear increase with respect to the number of users. It is thus of great interest to develop schemes which can reduce the numbers of users and/or bits to be fed back. The idea of using only one-bit feedback is introduced in several works, e.g., [36] [37] [38]. In this scheme, the user sends "1" when the SINR value is above a pre-determined threshold, and "0" vice-versa. Since the performance of OBF/RBF only depends on the favourable channels, one bit of feedback per user can capture almost all gain available due to the multi-user diversity. Optimal quantization strategy for OBF systems with more than one bit feedback is proposed in [36]. It is also worth noting the group random access-based feedback scheme in [39] and the multi-user diversity/throughput tradeoff analysis in [40]. The main tool to study the performance of OBF/RBF under reduced feedback schemes is the large-number-of-users analysis.

3.4. Non-orthogonal RBF and Grassmanian line packing problem

Denote the space of unit-norm transmit beamforming vectors in $\mathbb{C}^{N_T \times 1}$ as $\mathbb{O}(N_T, 1)$. A distance function of $\boldsymbol{v}_1, \boldsymbol{v}_2 \in \mathbb{O}(N_T, 1)$ can be defined to be the sine of the angle between them [41]

$$d(v_1, v_2) = sin(v_1, v_2) = \sqrt{1 - |v_1^H v_2|^2}, \tag{27}$$

which is known as the chordal distance. The problem of finding the packing of M unit-norm vectors in $\mathbb{C}^{N_T \times 1}$ that has the maximum minimum distance between any pair of them is called the *Grassmannian line packing problem* (GLPP). The GLPP appears in the problem of designing beamforming codebook for space-time codes [42] [43].

Given that the number of transmit beams is less than or equal to the number of transmit antennas, i.e., $M \leq N_T$, any orthonormal set $\{\boldsymbol{\phi}_m\}_{m=1}^{M}$ is a solution of the GLPP. However, assuming that the BS sends $M > N_T$ beams to serve more users simultaneously and improve the fairness of the system, finding $\{\boldsymbol{\phi}_m\}_{m=1}^{M}$ is a nontrivial GLPP. The idea of using more than N_T beams is first proposed in [44] with $M = N_T + 1$, and further studied in [45]. Zorba *et. al.* argue that the scaling law $M \log_2 \log K$ is still true for $M = N_T + 1$ case [44], while the results in [45] imply that non-orthogonal beamforming matrix induces an interference-limited effect on the sum rate, and the multi-user diversity vanishes. Since both studies are based on approximated derivations, more rigorous investigations are necessary before any conclusion is drawn.

3.5. Other studies

Beam selection and beam power control algorithms for single-cell RBF are proposed in [46] [47] [33] [48]. The objective is to improve the rate performance especially when the number of users is not so large. The idea of employing a codebook of predetermined orthonormal beamforming matrices is introduced in [30] [31] [27]. While [30] [31] investigate RBF when quantized, normalized channel vectors are fed back to the BS, [49] studies the codebook design problem and the rate performance assuming that opportunistic selection is also performed on the codebook. These problems are related to Section 3.3 and the GLPP in Section 3.4. Fairness scheduling problem is studied in [19], in which the "*proportional fair scheduling* (PFS)" scheme is proposed. It is not surprising that most of the later developments approach PFS from a network layer's perspective. Notably, the convergence of PFS algorithm for many-user cases under general network conditions is proved in [50], and a global PFS for multi-cell systems is introduced in [51].

4. Multi-cell RBF: Finite-SNR analysis

4.1. Multi-cell MISO RBF

In this subsection, we review the recent results on the achievable sum rate of the multi-cell MISO RBF scheme under finite-SNR regime [22]. In particular, we first consider an extension of Lemma 3.1 to the multi-cell case subject to the ICI, and furthermore show the asymptotic sum-rate scaling law as the number of users per cell tends to infinity.

For the single-cell RBF case, the SINR distributions given in (17) and (18) are obtained in [20]. The following lemma establishes similar results for the multi-cell case

Lemma 4.1. *([22, Lemma 3.2], see also Section 4.2) In the multi-cell MISO RBF, the PDF and CDF of the SINR $S := SINR_{k,m}^{(c)}$, $\forall k, m$, have closed-form expressions given by*

$$f_S^{(c)}(s) = \frac{e^{-s/\eta_c}}{(s+1)^{M_c-1}\prod_{l=1,l\neq c}^{C}\left(\frac{\mu_{l,c}}{\eta_c}s+1\right)^{M_l}}\left[\frac{1}{\eta_c}+\frac{M_c-1}{s+1}+\sum_{l=1,l\neq c}^{C}\frac{M_l}{s+\frac{\eta_c}{\mu_{l,c}}}\right], \tag{28}$$

$$F_S^{(c)}(s) = 1-\frac{e^{-s/\eta_c}}{(s+1)^{M_c-1}\prod_{l=1,l\neq c}^{C}\left(\frac{\mu_{l,c}}{\eta_c}s+1\right)^{M_l}}. \tag{29}$$

4.1.1. Sum rate with finite K

With Lemma 4.1, Lemma 3.1 is readily generalized to the multi-cell case in the following theorem.

Theorem 4.1. *([22, Theorem 3.1]) The total sum rate of a C-cell MISO RBF system equals to $\sum_{c=1}^{C} R_{RBF}^{(c)}$, in which the individual sum rate of the c-th cell, $R_{RBF}^{(c)}$, is given by*

$$\begin{aligned}R_{RBF}^{(c)} = \frac{M_c}{\log 2}\sum_{n=1}^{K_c}(-1)^n\binom{K_c}{n}\prod_{l=1,l\neq c}^{C}\left(\frac{\eta_c}{\mu_{l,c}}\right)^{nM_l}\times\\ \left\{\sum_{p=1}^{n(M_c-1)+1}\frac{A_{n,c,p}}{(p-1)!}\left[e^{\frac{n}{\eta_c}}\left(-\frac{n}{\eta_c}\right)^{p-1}Ei\left(-\frac{n}{\eta_c}\right)-\sum_{m=1}^{p-1}\left(-\frac{n}{\eta_c}\right)^{m-1}(p-1-m)!\right]\right.\\ +\sum_{l=1,l\neq c}^{C}\sum_{q=1}^{nM_l}\frac{A_{n,l,q}}{(q-1)!}\left[e^{\frac{n}{\mu_{l,c}}}\left(-\frac{n}{\eta_c}\right)^{q-1}Ei\left(-\frac{n}{\mu_{l,c}}\right)\right.\\ \left.\left.-\sum_{m=1}^{q-1}\left(-\frac{n}{\eta_c}\right)^{m-1}\left(\frac{\mu_{l,c}}{\eta_c}\right)^{q-m}(q-1-m)!\right]\right\},\end{aligned} \tag{30}$$

where $A_{n,c,p}$'s and $A_{n,l,q}$'s are the coefficients from the following partial fractional decomposition:

$$\frac{1}{(x+1)^{n(M_c-1)+1}\prod_{l\neq c}^{C}\left(x+\frac{\eta_c}{\mu_{l,c}}\right)^{nM_l}} = \sum_{p=1}^{n(M_c-1)+1}\frac{A_{n,c,p}}{(x+1)^p}+\sum_{l=1,l\neq c}^{C}\sum_{q=1}^{nM_l}\frac{A_{n,l,q}}{\left(x+\frac{\eta_c}{\mu_{l,c}}\right)^q}, \tag{31}$$

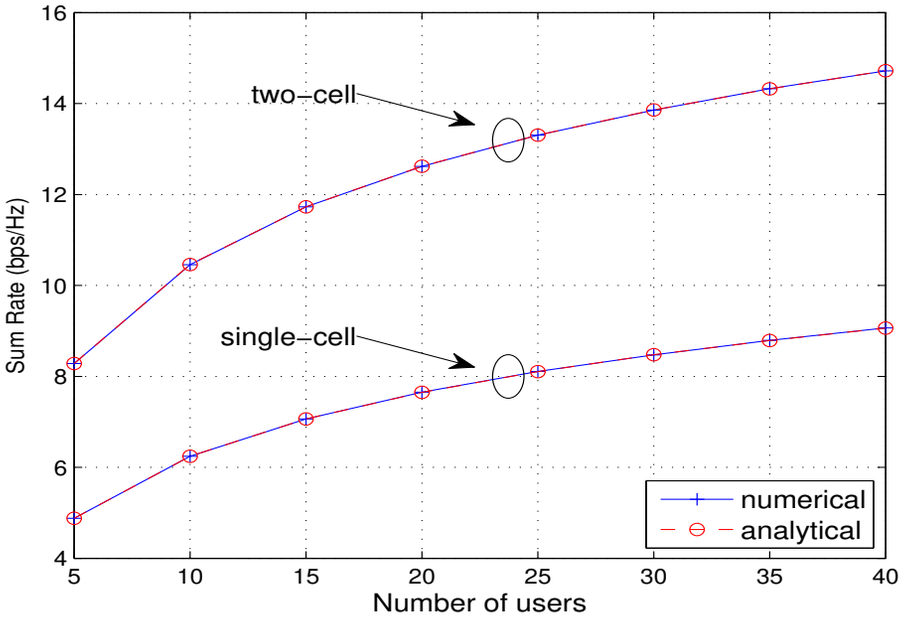


Figure 1. Comparison of the analytical and numerical results on the RBF sum rate.

and thus given by [52, (2.102)]:

$$A_{n,c,p} = \frac{1}{(n(M_c-1)-p+1)!}\frac{d^{n(M_c-1)-p+1}}{dx^{n(M_c-1)-p+1}}\left[\frac{1}{\prod_{l\neq c}^{C}\left(x+\frac{\eta}{\mu_l}\right)^{nM_l}}\right]\Bigg|_{x=-1}, \tag{32}$$

$$A_{n,l,q} = \frac{1}{(nM_l-q)!}\frac{d^{nM_l-q}}{dx^{nM_l-q}}\left[\frac{1}{(x+1)^{n(M_c-1)+1}\prod_{t\neq l,c}^{C}\left(x+\frac{\eta}{\mu_t}\right)^{nM_t}}\right]\Bigg|_{x=-\eta_c/\mu_{l,c}}. \tag{33}$$

If the original feedback scheme in [20] is employed, (30) becomes a close approximation of the c-th sum rate. Note that no other results than Theorem 4.1 are available in the literature for the multi-cell RBF sum rate.

Fig. 1 shows the analytical and numerical results on the RBF sum rate as a function of the number of users for both single-cell and two-cell systems. In the single-cell case, $M = N_T = 3$, $\eta = 20$ dB, while in the two-cell case, $K_1 = K_2$, $M_1 = M_2 = N_T = 3$, $\eta_1 = \eta_2 = 20$ dB, $\mu_{2,1} = 6$ dB, and $\mu_{1,2} = 10$ dB. It is observed that the sum-rate expressions in (19) and (30) are very accurate. Thus, it is possible to use Theorem 4.1 to compute all the sum-rate tradeoffs among different cells in a multi-cell RBF system, which leads to the achievable rate region. However, such a characterization requires intensive computations, and does not provide any useful insights.

4.1.2. Asymptotic sum rate as $K_c \to \infty$

An attempt to extend the famous scaling law $M \log_2 \log K$ to the multi-cell RBF case has been made in [53] based on an approximation of the SINR's PDF (which is applicable if

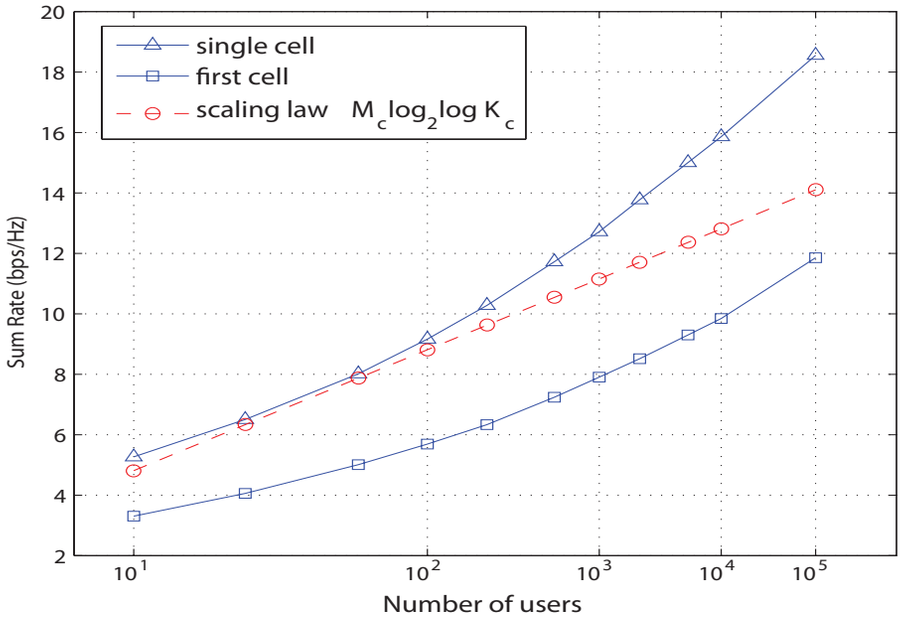


Figure 2. Comparison of the numerical sum rate and the sum-rate scaling law for RBF.

the SNR and INRs are all roughly equal), by showing that the same asymptotic sum-rate $M_c \log_2 \log K_c$ for each individual cell holds as the single-cell case. However, we note that with the exact SINR distributions in Lemma 4.1, a rigorous proof can be obtained, leading to the following proposition.

Proposition 4.1. *([22, Proposition 3.1]) For fixed M_c's and P_T, $c = 1, \cdots, C$, we have*

$$\lim_{K_c \to \infty} \frac{R_{RBF}^{(c)}}{M_c \log_2 \log K_c} = 1. \tag{34}$$

Fig. 2 depicts both the numerical and theoretical asymptotic sum-rates for a single-cell RBF system, and the first cell of a two-cell RBF system. In the single-cell case, $\eta = 10$ dB, and $M = N_T = 4$, while in the two-cell case, $M_1 = M_2 = N_T = 4$, $\eta_1 = 10$ dB, and $\mu_{2,1} = 6$ dB. We observe that the convergence to the sum-rate scaling law $M_c \log_2 \log K_c$ is rather slow in both cases. For example, even with K or K_c to be 10^5, the convergence is still not clear. In fact, Fig. 2 indicates that the sum-rate might follow a (single-) logarithmically scaling law. Furthermore, Proposition 4.1 implies that the sum-rate scaling law $M_c \log_2 \log K_c$ holds for any cell regardless of the ICI as $K_c \to \infty$. As a consequence, this result implies that each cell should apply the maximum number of transmit beams, i.e., $M_c = N_T, \forall c$, to maximize the per-cell throughput. Such a conclusion may be misleading in a practical multi-cell system with non-negligible ICI. The above two main drawbacks, namely, slow convergence and misleading conclusion, limit the usefulness of the conventional sum-rate scaling law $M_c \log_2 \log K_c$ for the multi-cell RBF.

http://dx.doi.org/10.5772/57131

4.2. Multi-cell MIMO RBF

To study the achievable sum-rates of the RBF-Rx schemes, it is necessary to investigate the SINRs given in (7), (9), and (12). The following lemmas establish the SINR distributions in three cases.

Lemma 4.2. *([24, Corollary 3.1], see also [54]) Given $N_R \leq \sum_{l=1}^{C} M_l - 1$, the CDF of the random variable $S := SINR_{k,m}^{(MMSE,c)}$ in (7) is*

$$F_S(s) = 1 - \frac{e^{-s/\eta_c} \left(\sum_{i=0}^{N_R-1} \zeta_i s^i \right)}{(1+s)^{M_c-1} \prod_{l=1,l\neq c}^{\sum M_c - 1} (1 + \frac{\mu_{l,c}}{\eta_c} s)^{M_l}}, \tag{35}$$

in which ζ_i is the coefficient of s^i in the product $(1+s)^{M_c-1} \prod_{l=1,l\neq c}^{\sum M_c-1} (1 + \frac{\mu_{l,c}}{\eta_c} s)^{M_l}$.

Lemma 4.3. *([24, Theorem 3.2]) The CDF of $S := SINR_{k,m}^{(MF,c)}$ can be expressed as*

$$F_S(s) = 1 - e^{-s/\eta_c} \sum_{k=0}^{N_R-1} \sum_{j=0}^{k} \frac{(-1)^j s^k}{(k-j)!j!\eta_c^{k-j}} \frac{d^j T_0}{ds^j}, \tag{36}$$

in which

$$T_0 = \frac{1}{(1+s)^{M_c-1} \prod_{l=1,l\neq c}^{C} (1 + \frac{\mu_{l,c}}{\eta_c} s)^{M_l}}. \tag{37}$$

Lemma 4.4. *([24, Corollary 3.2]) The CDF of $S := SINR_{k,m}^{(AS,c)}$ can be expressed as*

$$F_S(s) = \left(1 - \frac{e^{-s/\eta_c}}{(s+1)^{M_c-1} \prod_{l=1,l\neq c}^{C} \left(\frac{\mu_{l,c}}{\eta_c} s + 1 \right)^{M_l}} \right)^{N_R}. \tag{38}$$

In Fig. 3, we present the per-cell SINR CDFs of the RBF-MMSE, RBF-MF, and RBF-AS with the following setup: $C = 4$, $\eta_1 = 20$ dB, $N_R = 3$, $M_1 = 3$, $[\mu_{2,1}, \mu_{3,1}, \mu_{4,1}] = [0, -3, 3]$ dB, and $[M_2, M_3, M_4] = [3, 2, 4]$. The numerical results are obtained with Monte-Carlo simulations, while the analytical results are computed based on Lemma 4.2, 4.3, and 4.4. As a reference, we also present the numerical CDF of the MISO RBF with single-antenna users. It is observed that spatial receive diversity does help improving the SINR performance. However, only in the RBF-MMSE scheme that there exists a tremendous gain. Finally, we note that the SINR performance of the RBF-MF is *not* always better than that of the RBF-AS.

With Lemma 4.2, 4.3, and 4.4, it is possible to extend Theorem 4.1 to multi-cell MIMO RBF systems. The results posses complicated expressions and, again, does not lead to useful insights. We are more interested in the following proposition

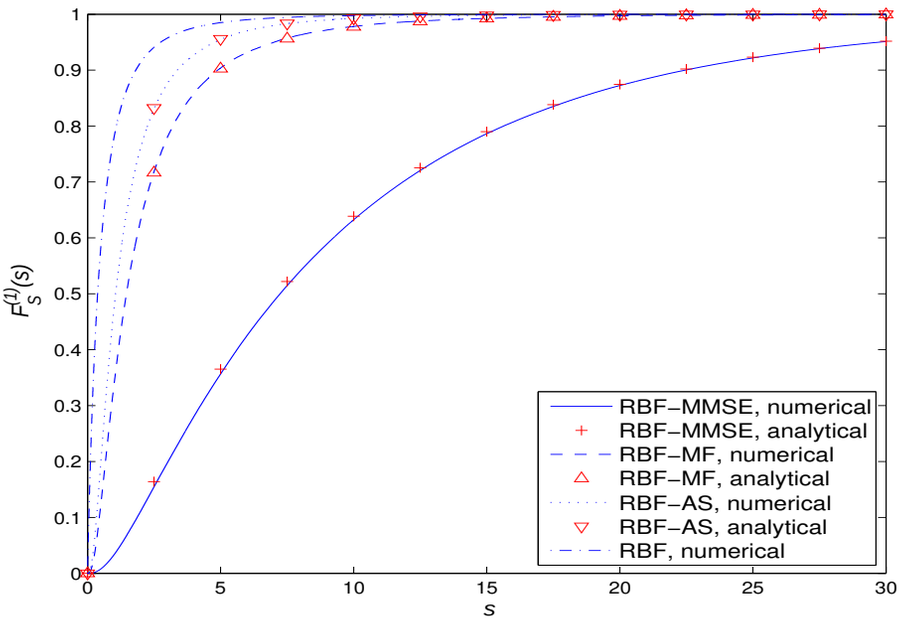


Figure 3. Comparison of the numerical and analytical CDFs of the per-cell SINR.

Proposition 4.2. *([24, Proposition 4.2]) For fixed M_c, N_R and P_T, $c = 1, \cdots, C$, we have*

$$\lim_{K_c \to \infty} \frac{R_{RBF\text{-}Rx}^{(c)}}{M_c \log_2 \log K_c} = 1, \tag{39}$$

where "Rx" denotes any receive diversity scheme at the users, e.g., MMSE, MF, or AS.

Essentially, this proposition extends Proposition 4.1 to the multi-cell MIMO case. Note that a similar result for a single-cell setup is obtained in [20] [21]. The proposition implies that spatial receive diversity only provides *marginal* gain to the rate performance of multi-cell MIMO RBF systems. However, as shown in Section 4.1.2, the traditional asymptotic analysis might not accurately characterize the RBF sum-rate in the condition of a small number of users (even up to K, $K_c = 10^5$). This negative conclusion on the receive diversity, therefore, might be misleading. The benefit of receive diversity to multi-cell RBF systems will be discussed further in Section 5.2.

5. Multi-cell RBF: High-SNR analysis and the degrees of freedom region

Motivated by the major limitations of the finite-SNR analysis, [22] and [23] propose using the high-SNR/DoF analysis to study the rate performance of multi-cell/IC systems with opportunistic scheduling. In particular, the multi-cell MISO RBF and ad-hoc SISO IC are considered in [22] and [23], respectively. A further extension is [24], in which the multi-cell MIMO RBF schemes are investigated to reveal the benefit of receive diversity. It has been shown that the high-SNR/DoF analysis provides a succinct description of the interplay between the multi-user diversity, spatial receive diversity and spatial multiplexing gains achievable in RBF.

http://dx.doi.org/10.5772/57131

In this section, we introduce the high-SNR/DoF analysis and the studies on multi-cell MISO/MIMO RBF. We first specify the DoF region, which was defined in [9] and is restated below for convenience.

Definition 5.1. *(General DoF region) The DoF region of a C-cell MIMO-BC system is defined as*

$$\mathcal{D}_{MIMO} = \Bigg\{ (d_1, d_2, \cdots, d_C) \in \mathbb{R}_+^C : \forall (\omega_1, \omega_2, \cdots, \omega_C) \in \mathbb{R}_+^C; \sum_{c=1}^{C} \omega_c d_c \leq \lim_{\rho \to \infty} \sup_{\boldsymbol{R} \in \mathcal{R}} \sum_{c=1}^{C} \omega_c \frac{R_{sum}^{(c)}}{\log_2 \rho} \Bigg\}, \tag{40}$$

where ρ is the per-cell SNR; ω_c, d_c, and $R_{sum}^{(c)}$ are the non-negative rate weight, the achievable DoF, and the sum rate of the c-th cell, respectively; and the region $\mathcal{R}$ is the set of all the achievable sum-rate tuples for all the cells, denoted by $\boldsymbol{R} = (R_{sum}^{(1)}, R_{sum}^{(2)}, \cdots, R_{sum}^{(C)})$.

If the multi-cell MIMO RBF schemes are deployed, the achievable DoF region defined in (40) is reduced to

Definition 5.2. *(DoF region with RBF) The DoF region of a C-cell MIMO RBF system is defined as*

$$\mathcal{D}_{RBF\text{-}Rx} = \Bigg\{ (d_1, d_2, \cdots, d_C) \in \mathbb{R}_+^C : \forall (\omega_1, \omega_2, \cdots, \omega_C) \in \mathbb{R}_+^C; \sum_{c=1}^{C} \omega_c d_c \leq \lim_{\rho \to \infty} \left[\max_{M_c \in \{0, \cdots, N_T\}} \sum_{c=1}^{C} \omega_c \frac{R_{RBF\text{-}Rx}^{(c)}}{\log_2 \rho} \right] \Bigg\}. \tag{41}$$

in which "Rx" denotes either MMSE, MF or AS.

Furthermore, the DoF regions are denoted as $\mathcal{D}_{\text{MISO}}$ and $\mathcal{D}_{\text{RBF}}$, respectively, under a multi-cell MISO setup. Certainly, $\mathcal{D}_{\text{RBF}} \subseteq \mathcal{D}_{\text{MISO}}$ and $\mathcal{D}_{\text{RBF-Rx}} \subseteq \mathcal{D}_{\text{MIMO}}$.

Note that the DoF region is, in general, applicable for any number of users per cell, K_c. However, if it is assumed that all K_c's are constant with $\rho \to \infty$, it can be shown that the DoF regions for the multi-cell RBF schemes given in (41) will collapse to the null point, i.e., a zero DoF for all the cells, due to the intra-/inter-cell interference[2]. It thus follows that for the analytical tractability, the DoF region characterization for the multi-cell RBF requires that K_c increases in a certain order with the SNR, ρ. [24] [22] thus make the following assumption[3]:

Assumption 1. *The number of users in each cell scales with ρ in the order of ρ^{α_c}, with $\alpha_c \geq 0$, denoted by $K_c = \Theta(\rho^{\alpha_c}), c = 1, \ldots, C$, i.e., $K_c/\rho^{\alpha_c} \to \delta$ as $\rho \to \infty$, with δ being a positive constant independent of α_c.*

[2] A rigorous proof of this claim can be deduced from Theorem 5.2 and 5.3 later for the special case of $\alpha_c = 0$, $\forall c$, i.e., all cells having a constant number of users.

[3] In [23], Tajer *et. al.* consider a more general assumption on the number of ad-hoc SISO links n, i.e., $\frac{\log n}{\log \rho} \to \alpha$ with $\alpha > 0$.

Considering the number of per-cell users to scale polynomially with the SNR is general as well as convenient. The linear scaling law, i.e., $K_c = \beta_c \rho$, with constant $\beta_c > 0$, is only a special case of $K_c = \Theta(\rho^{\alpha_c})$ with $\alpha_c = 1$; if K_c is a constant, then the corresponding α_c is zero. As will be shown later in this section, Assumption 1 enables us to obtain an efficient as well as insightful characterization of the DoF region for the multi-cell RBF. Note that the DoF region under Assumption 1 can be considered as a generalization of the conventional DoF region analysis based on IA [9] for the case of finite number of users, to the case of asymptotically large number of users that scales with the SNR. For the notational convenience, we use $\mathcal{D}_{\text{MISO}}(\boldsymbol{\alpha})$, $\mathcal{D}_{\text{MIMO}}(\boldsymbol{\alpha})$, $\mathcal{D}_{\text{RBF}}(\boldsymbol{\alpha})$, and $\mathcal{D}_{\text{RBF-Rx}}(\boldsymbol{\alpha})$ to denote the achievable DoF regions corresponding to $K_c = \Theta(\rho^{\alpha_c})$, $c = 1, \cdots, C$, and $\boldsymbol{\alpha} = [\alpha_1, \cdots, \alpha_C]^T$.

5.1. Multi-cell MISO RBF

In this subsection, we review the MISO RBF study in [22]. It is revealed that the high-SNR analysis provides an efficient way of characterizing the achievable sum rate for RBF, even for small values of SNR and number of users. In single-cell RBF, the DoF result shows that adjusting the number of beams according to the number of users can improve the achievable sum rate, thus providing a theoretical explanation for observations in, e.g., [46] [33] [48]. Extending to the multi-cell case, it is furthermore unfolded that collaboration among the BSs in assigning their respective numbers of data beams based on different per-cell user densities is essential to achieve the optimal throughput tradeoffs among different cells.

5.1.1. Single-cell case

First, we consider the DoF for the achievable sum rate in the single-cell RBF case without the ICI. The cell index c in (2) thus is dropped for brevity. In the single-cell case, the DoF region collapses to a line, bounded by 0 and $d^*_{\text{RBF}}(\alpha)$, where $d^*_{\text{RBF}}(\alpha) \geq 0$ denotes the maximum DoF achievable for the RBF sum rate.

The achievable DoF for single-cell RBF is defined with a given pair of α and M as

$$d_{\text{RBF}}(\alpha, M) = \lim_{\rho \to \infty} \frac{R_{\text{RBF}}}{\log_2 \rho} = \lim_{\eta \to \infty} \frac{R_{\text{RBF}}}{\log_2 \eta} \tag{42}$$

since $\eta = \rho / M$. Thus, $d^*_{\text{RBF}}(\alpha) = \max_{M \in \{1, \cdots, N_T\}} d_{\text{RBF}}(\alpha, M)$ for a given $\alpha \geq 0$. The DoF $d_{RBF}(\alpha, M)$ is characterized in the following lemma.

Lemma 5.1. *([22, Lemma 4.1]) Assuming $K = \Theta(\rho^{\alpha})$, the DoF of single-cell MISO RBF with $M \leq N_T$ orthogonal transmit beams is given by*

$$d_{RBF}(\alpha, M) = \begin{cases} \dfrac{\alpha M}{M-1}, & 0 \leq \alpha \leq M-1, \quad (43a) \\ M, & \alpha > M-1. \quad (43b) \end{cases}$$

With RBF and under the assumption $K = \Theta(\rho^{\alpha})$, it is interesting to observe from Lemma 5.1 that the achievable DoF can be a non-negative real number (as compared to the conventional

http://dx.doi.org/10.5772/57131

integer DoF in the literature with a finite K). Moreover, it is observed that for any given $0 < \alpha < N_T - 1$, assigning more transmit beams by increasing M initially improves the sum-rate DoF if $M \leq \alpha + 1$; however, as $M > \alpha + 1$, the DoF may not necessarily increase with M due to the more dominant inter-beam/intra-cell interference. Note that the term $M-1$ in the denominator of (43a) is exactly the number of interfering beams to one particular beam. Thus, Lemma 5.1 provides a succinct description of the interplay between the available multi-user diversity (specified by α with a larger α denoting a higher user density or the number of users in a cell), the level of the intra-cell interference (specified by $M-1$), and the achievable spatial multiplexing gain or DoF, $d_{\mathrm{RBF}}(\alpha, M)$.

It is also of great interest to obtain the maximum achievable DoF for a given α. The result is shown in the following theorem.

Theorem 5.1. *([22, Theorem 4.1]) For the single-cell MISO RBF with N_T transmit antennas and user density coefficient α, the maximum achievable DoF and the corresponding optimal number of transmit beams are*[4]

$$d^*_{RBF}(\alpha) = \begin{cases} \lfloor \alpha \rfloor + 1, & \alpha \leq N_T - 1, 1 \geq \{\alpha\}(\lfloor \alpha \rfloor + 2), \\ \frac{\alpha(\lfloor \alpha \rfloor + 2)}{\lfloor \alpha \rfloor + 1}, & \alpha \leq N_T - 1, \{\alpha\}(\lfloor \alpha \rfloor + 2) > 1, \\ N_T, & \alpha > N_T - 1. \end{cases} \tag{44}$$

$$M^*_{RBF}(\alpha) = \begin{cases} \lfloor \alpha \rfloor + 1, & \alpha \leq N_T - 1, 1 \geq \{\alpha\}(\lfloor \alpha \rfloor + 2), \\ \lfloor \alpha \rfloor + 2, & \alpha \leq N_T - 1, \{\alpha\}(\lfloor \alpha \rfloor + 2) > 1, \\ N_T, & \alpha > N_T - 1. \end{cases} \tag{45}$$

In Fig. 4, we compare the numerical sum rate and the analytical scaling law in Lemma 5.1. It is observed that the newly obtained sum-rate scaling law, $R_{\mathrm{RBF}} \approx d_{\mathrm{RBF}}(\alpha, M) \log_2 \rho$, in the single-cell RBF case is very accurate, even for small values of SNR ρ and number of users $K = \lfloor \rho^{\alpha} \rfloor$. Compared with Fig. 2 for the conventional scaling law, $R_{\mathrm{RBF}} \approx M \log_2 \log K$, a much faster convergence is observed here. The DoF approach thus provides a more efficient way of characterizing the achievable sum rate for single-cell RBF. Also observe that the sum rate for $M = 2$ is higher than that for $M = 4$. This is because with $N_T = 4$ and $\alpha = 1$ in this example, the optimal number of beams to achieve $d^*_{RBF}(1) = 2$ is $M^*_{RBF}(1) = 2$ from (45). Since many previous studies have observed that adjusting the number of beams according to the number of users in single-cell RBF can improve the achievable sum rate (see, e.g., [46] [33] [48]), our study here can be considered as a theoretical explanation for such an observation.

Fig. 5 shows the maximum DoF and the corresponding optimal number of transmit beams versus the user density coefficient α with $N_T = 4$ for single-cell RBF, according to Theorem 5.1. It is observed that to maximize the achievable sum rate, we should only transmit more data beams when the number of users increases beyond a certain threshold. It is also observed that the maximum DoF $d^*_{RBF}(\alpha) = 4$ with $M = N_T = 4$ is attained when $\alpha \geq 3$ since $M^*_{RBF}(3) = 4$.

[4] The notations $\lfloor \alpha \rfloor$ and $\{\alpha\}$ denote the integer and fractional parts of a real number α, respectively.

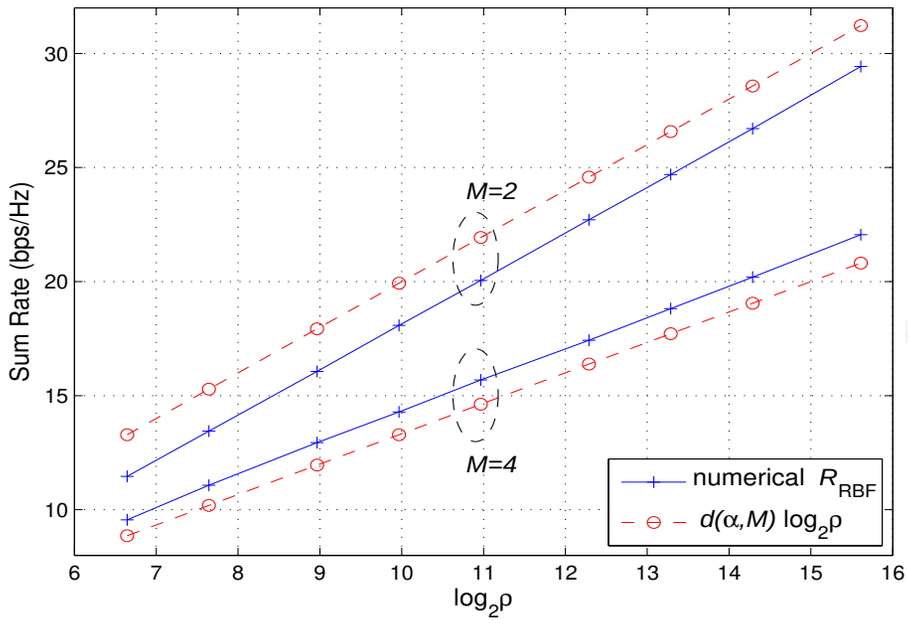


Figure 4. Comparison of the numerical sum rate and the scaling law $d_{RBF}(\alpha, M)\log_2\rho$, with $N_T = 4$, $\alpha = 1$, and $K = \lfloor \rho^{\alpha} \rfloor$.

5.1.2. Multi-cell case

We then extend the high-SNR analysis for the single-cell RBF to the more general multi-cell RBF subject to the ICI. For convenience, we denote the achievable sum-rate DoF of the c-th cell as $d_{\mathrm{RBF},c}(\alpha_c, \boldsymbol{m}) = \lim_{\rho\to\infty} \frac{R_{\mathrm{RBF}}^{(c)}}{\log_2\rho}$, where $\boldsymbol{m} = [M_1,\cdots,M_C]^T$ is a given set of numbers of transmit beams at different BSs. We then state the next lemma on the achieve DoF of the c-th cell.

Lemma 5.2. *([22, Lemma 4.2]) In the multi-cell MISO RBF, assuming $K_c = \Theta(\rho^{\alpha_c})$, the achievable DoF of the c-th cell $d_{RBF,c}(\alpha_c, \boldsymbol{m})$, $c \in \{1,\ldots,C\}$, for a given $\boldsymbol{m}$ is*

$$d_{RBF,c}(\alpha_c, \boldsymbol{m}) = \begin{cases} \dfrac{\alpha_c M_c}{\sum_{l=1}^{C} M_l - 1}, & 0 \le \alpha_c \le \sum_{l=1}^{C} M_l - 1, \quad (46a) \\ M_c, & \alpha_c > \sum_{l=1}^{C} M_l - 1. \quad (46b) \end{cases}$$

Similar to Lemma 5.1 for the single-cell case, Lemma 5.2 reveals the relationship among the multi-user diversity, the level of the interference, and the achievable DoF for multi-cell RBF. However, as compared to the single-cell case, there are not only $M_c - 1$ intra-cell interfering beams, but also $\sum_{l=1,l\neq c}^{C} M_l$ inter-cell interfering beams for any beam of the c-th cell in the multi-cell case, as observed from the denominator in (46a), which results in a decrease in the achievable DoF per cell.

Next, we obtain characterization of the DoF region defined in (41) for the multi-cell RBF with any given set of per-cell user density coefficients, denoted by $\boldsymbol{\alpha} = [\alpha_1, \cdots, \alpha_C]^T$ in the following theorem; for convenience, we denote $\boldsymbol{d}_{\mathrm{RBF}}(\boldsymbol{\alpha}, \boldsymbol{m}) = \left[d_{\mathrm{RBF},1}(\alpha_1, \boldsymbol{m}), \cdots, d_{RBF,C}(\alpha_C, \boldsymbol{m}) \right]^T$, with $d_{\mathrm{RBF},c}(\alpha_c, \boldsymbol{m})$ given in Lemma 5.2.

http://dx.doi.org/10.5772/57131

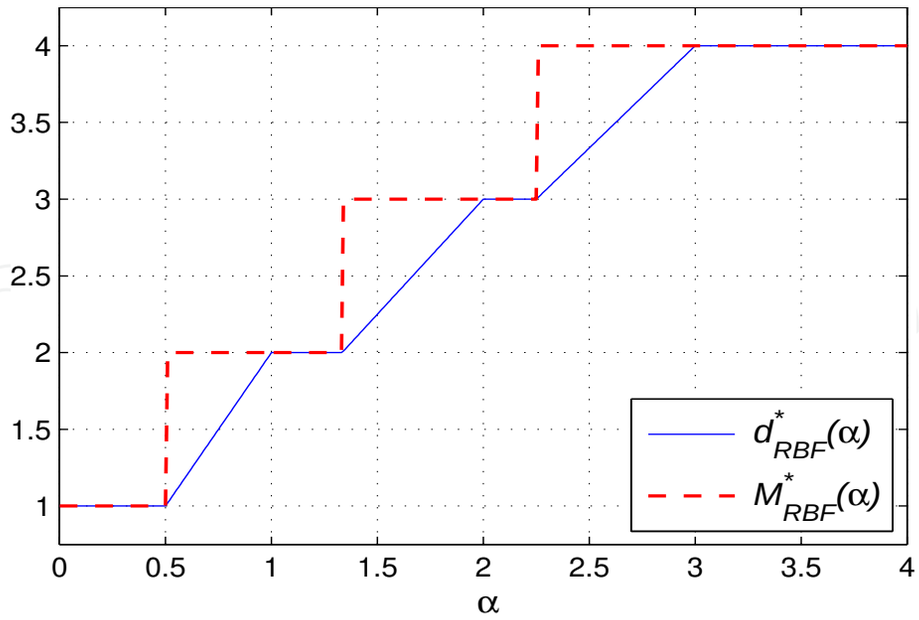


Figure 5. The maximum DoF $d^*_{RBF}(\alpha)$ and optimal number of beams $M^*_{RBF}(\alpha)$ with $N_T = 4$.

Theorem 5.2. *([22, Theorem 4.2]) Assuming $K_c = \Theta\left(\rho^{\alpha_c}\right), c = 1, \ldots, C$, the achievable DoF region of a C-cell RBF system is given by*

$$\mathcal{D}_{RBF}(\boldsymbol{\alpha}) = \boldsymbol{conv}\left\{\boldsymbol{d}_{RBF}(\boldsymbol{\alpha}, \boldsymbol{m}), M_c \in \{0, \cdots, N_T\},\ c = 1, \cdots, C\right\}, \tag{47}$$

*where **conv** denotes the convex hull operation.*

This theorem implies that we can obtain the DoF region of multi-cell RBF $\mathcal{D}_{\mathrm{RBF}}(\boldsymbol{\alpha})$ by taking the convex hull over all achievable DoF points $\boldsymbol{d}_{\mathrm{RBF}}(\boldsymbol{\alpha}, \boldsymbol{m})$ with all different values of $\boldsymbol{m}$, i.e., different BS beam number assignments.

In Fig. 6, we depict the DoF region of a two-cell RBF system with $N_T = 4$, and for different user density coefficients α_1 and α_2. The vertices of these regions can be obtained by setting appropriate numbers of beams $0 \leq M_1 \leq 4$ and $0 \leq M_2 \leq 4$, while time-sharing between these vertices yields the entire boundary. To achieve the maximum sum-DoF of both cells, it is observed that a rule of thumb is to transmit more beams in the cell with a higher user density, and when α_1 and α_2 are both small, even turn off the BS of the cell with the smaller user density. Since the maximum sum-DoF does not consider the throughput fairness, the DoF region clearly shows all the achievable sum-rate tradeoffs among different cells, by observing its (Pareto) boundary as shown in Fig. 6. It is also observed that switching the two BSs to be on/off alternately achieves the optimal DoF boundary when the numbers of users in both cells are small, but is strictly suboptimal when the user number becomes large (see the dashed line in Fig. 6).

Furthermore, consider the case without any cooperation between these two BSs in assigning their numbers of transmit beams, i.e., both cells act selfishly by transmitting $M_c = N_T$ beams to intend to maximize their own DoF. The resulted DoF pairs $\boldsymbol{d}_{\mathrm{RBF}}([\alpha_1, \alpha_2], [4, 4])$ for three

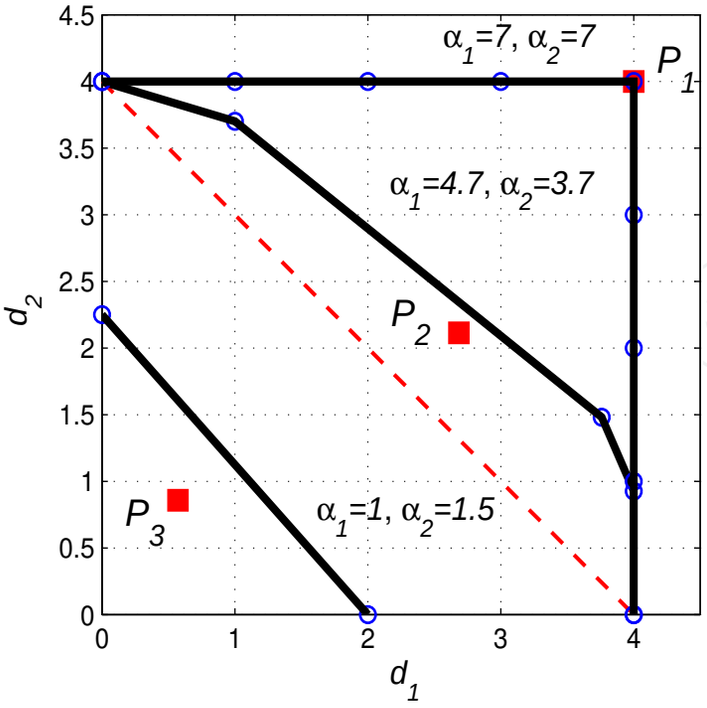


Figure 6. DoF region of two-cell RBF system with $N_T = 4$.

sets of $\boldsymbol{\alpha}$ are shown in Fig. 6 as P_1, P_2, and P_3, respectively. It is observed that the smaller the user densities are, the further the above non-cooperative multi-cell RBF scheme deviates from the Pareto boundary. In general, the optimal DoF tradeoffs or the boundary DoF pairs are achieved when both cells cooperatively assign their numbers of transmit beams based on their respective user densities, especially when the numbers of users in both cells are not sufficiently large. Since the information needed to determine the optimal operating DoF point is only the individual cell user density coefficients, the DoF region provides a very useful method to globally optimize the coordinated multi-cell RBF scheme in practical systems.

5.2. Multi-cell MIMO RBF schemes: Benefit of spatial receive diversity

Spatial receive diversity is another topic which is not fully understood even in a single-cell RBF setup. As discussed in Section 4.2, RBF with and without receive diversity schemes still achieve the same sum-rate scaling law, assuming that the number of users per cell goes to infinity for any given user's SNR. Based on the conventional asymptotic analysis, it is thus concluded that receive diversity only provides *marginal* gain to the rate performance.

The objective of this subsection is to review the recent results on the rate performance of multi-cell MIMO RBF systems under the high-SNR/DoF analysis [24]. Contrasting with the large-number-of-users analysis, it is found that the benefit of receive diversity is significant for the RBF scheme. In particular, receive diversity introduces an interference mitigation effect on the DoF performance. As a consequence, an substantial less number of users in each cell is required to achieve a given DoF region comparing to the case without receive diversity. However, the gain is observed only with MMSE receiver but not with suboptimal

schemes such as MF or AS. This reflects a tradeoff between the rate/DoF performance and the complexity/delay time of RBF systems.

5.2.1. DoF of the c-th cell

Similarly to the MISO case, the DoF of the c-th RBF-Rx cell is defined as $d_{\text{RBF-Rx},c}(\alpha_c, \boldsymbol{m}) = \lim_{\rho\to\infty} \frac{R^{(c)}_{\text{RBF-Rx}}}{\log_2 \rho}$. We then obtain the DoF of the c-th cell.

Lemma 5.3. *([24, Lemma 4.1]) In the multi-cell RBF-MMSE, assuming $K_c = \Theta(\rho^{\alpha_c})$, the achievable DoF of the c-th cell $d_{RBF\text{-}MMSE,c}(\alpha_c, \boldsymbol{m})$, $c \in \{1, \ldots, C\}$, for a given $\boldsymbol{m}$ is*

$$d_{RBF\text{-}MMSE,c}(\alpha_c, \boldsymbol{m}) = \begin{cases} \dfrac{\alpha_c M_c}{\sum_{l=1}^{C} M_l - N_R}, & 0 \le \alpha_c \le \sum_{l=1}^{C} M_l - N_R, \quad (48a) \\ M_c, & \alpha_c > \sum_{l=1}^{C} M_l - N_R. \quad (48b) \end{cases}$$

Lemma 5.4. *([24, Lemma 4.2]) In the multi-cell RBF-MF/AS, assuming $K_c = \Theta(\rho^{\alpha_c})$, the achievable DoF of the c-th cell $d_{RBF\text{-}MF/AS,c}(\alpha_c, \boldsymbol{m})$, $c \in \{1, \ldots, C\}$, for a given $\boldsymbol{m}$ is*

$$d_{RBF\text{-}MF/AS,c}(\alpha_c, \boldsymbol{m}) = \begin{cases} \dfrac{\alpha_c M_c}{\sum_{l=1}^{C} M_l - 1}, & 0 \le \alpha_c \le \sum_{l=1}^{C} M_l - 1, \quad (49a) \\ M_c, & \alpha_c > \sum_{l=1}^{C} M_l - 1. \quad (49b) \end{cases}$$

The DoF scaling laws $d_{\text{RBF-MMSE},c}(\alpha_c, \boldsymbol{m}) \log_2 \rho$ and $d_{\text{RBF-MF/AS},c}(\alpha_c, \boldsymbol{m}) \log_2 \rho$ are compared in Fig. 7. As a reference, we also show the sum-rates of the RBF-MMSE, RBF-MF, and RBF-AS. Again, a good match is observed between the scaling law and the numerical results, even with small values of the SNR and number of users.

We first remark that the MMSE receiver produces an *interference mitigation* effect to the DoF performance. From Lemma 5.2 and 5.3, it is observed that $N_R - 1$ interferences can be effectively eliminated in the RBF-MMSE. In particular, with N_R degrees of freedom at the receiver, the users can use one for receiving signal and $N_R - 1$ for suppressing the interferences. Secondly, in terms of sum-rate, the gain captured by employing either RBF-MF or RBF-AS is only marginal comparing to the MISO RBF with single-antenna users, as shown in Lemma 5.4. The benefit of receive diversity, therefore, clearly depends on the availability of the interferences' CSI at the users. In the RBF-MMSE, this CSI is the interference-plus-noise covariance matrix $\boldsymbol{W}_k^{(c)}$. In fact, since there is no information about the interferences given to the users in the RBF-MF/AS, it is expected that no significant gain is achieved by these schemes comparing with the MISO RBF.

At this point, we observe a sharp contrast between the conclusions based on the high-SNR/DoF and large-number-of-users analysis. In the conventional analysis, Proposition 4.2 effectively implies that there is no significant rate gain for the multi-cell RBF with receive diversity scheme at the users, and also no loss with intra-/inter-cell interferences in the system as the number of users goes to infinity. Recalling the convergences of the two approaches, the high-SNR/DoF analysis, therefore, is a more efficient method

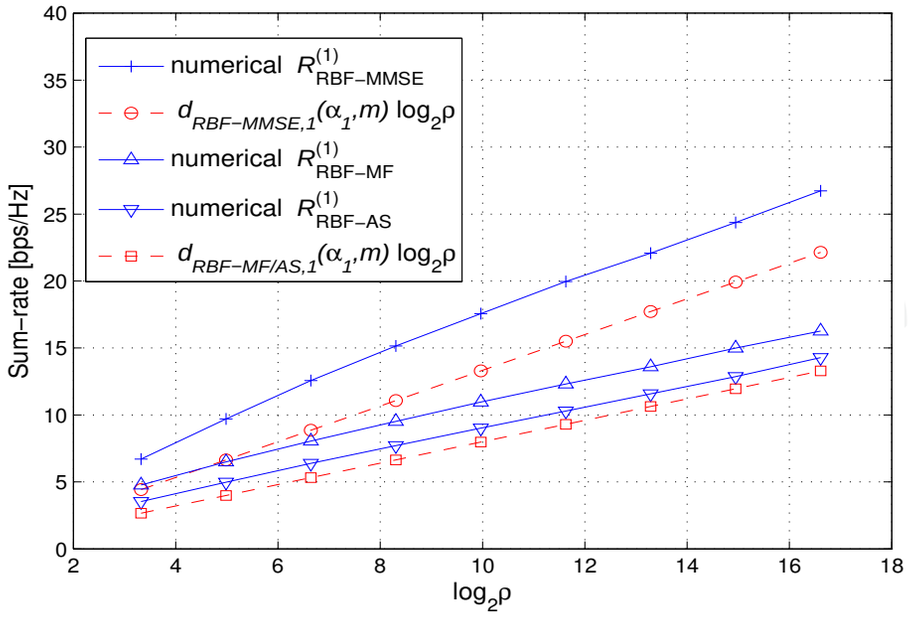


Figure 7. Comparison of the numerical sum-rate and the DoF scaling law, with $C = 2$, $[M_1, M_2] = [4, 2]$, $N_R = 3$, $\alpha_1 = 1$, $\gamma_{2,1} = -1$dB, and $K_1 = \lfloor \rho^{\alpha_1} \rfloor$.

of characterizing the achievable sum-rate for RBF under the effects of multi-user diversity, spatial receive diversity, and interference.

5.2.2. DoF region characterization

We denote $\boldsymbol{d}_{\text{RBF-Rx}}(\boldsymbol{\alpha}, \boldsymbol{m}) = \left[d_{\text{RBF-Rx},1}(\alpha_1, \boldsymbol{m}) \ , \cdots, \ d_{\text{RBF-Rx},C}(\alpha_C, \boldsymbol{m}) \right]^T$, with $d_{\text{RBF-Rx},c}(\alpha_c, \boldsymbol{m})$ given in Lemma 5.3 or 5.4. The characterization of the DoF region for the multi-cell RBF-Rx is given in the following theorem

Theorem 5.3. *Assuming $K_c = \Theta\left(\rho^{\alpha_c}\right), c = 1, \ldots, C$, the achievable DoF region of a C-cell RBF-Rx system is given by*

$$\mathcal{D}_{RBF\text{-}Rx}(\boldsymbol{\alpha}) = \boldsymbol{conv}\left\{ \boldsymbol{d}_{RBF\text{-}Rx}(\boldsymbol{\alpha}, \boldsymbol{m}), M_c \in \{0, \cdots, N_T\}, \ c = 1, \cdots, C \right\}, \tag{50}$$

*where **conv** denotes the convex hull operation and "Rx" stands for either MMSE, MF, or AS as usual.*

Fig. 8 depicts the DoF region of a two-cell system employing either the RBF-MMSE or RBF-MF/AS. We assume that $N_T = 4$, $N_R = 2$. The region's boundaries for RBF-MMSE and RBF-MF/AS are denoted by solid and dashed lines, respectively. When α_1 and α_2 are small, the DoF region is greatly expanded in the case of the RBF-MMSE. In fact, compared to the RBF-MF, RBF-AS, and MISO RBF, an *exponentially* less number of users in each cell is required to achieve a certain DoF region in the RBF-MMSE (see Lemma 5.3). The assistance of receive diversity to multi-user diversity, therefore, is significant.

We see that receive diversity is indeed beneficial for RBF systems. However, there exists a tradeoff between the rate/DoF performance and the complexity/delay time. The option thus

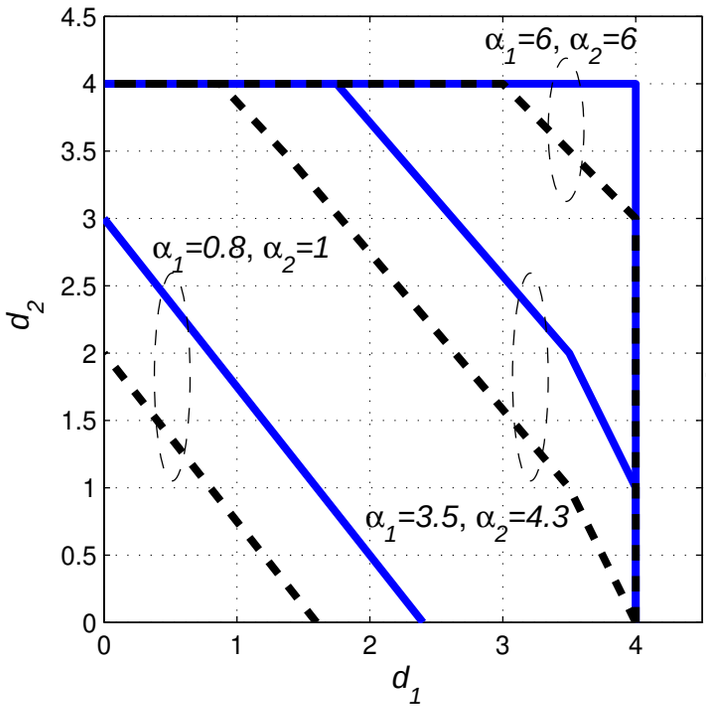


Figure 8. DoF regions of different RBF-MMSE and RBF-MF/AS systems.

depends on the communication system in consideration. The RBF-MMSE is a good choice if there are small numbers of users in the cells while the constrains on the complexity and delay time are slack. However, when the receivers are required to be simple and there are many users in the system, the RBF-MF, RBF-AS, or even MISO RBF, is more favourable.

5.3. Optimality of multi-cell RBF

So far, we have characterized the achievable DoF region for the multi-cell RBF schemes that require only partial CSI at the transmitter. One important question that remains unaddressed yet is how the multi-cell RBF performs as compared to the optimal transmission scheme (e.g., IA) for the multi-cell downlink system with the full transmitter CSI, in terms of achievable DoF region. In this subsection, we attempt to partially answer this question by focusing on the high-SNR/DoF regime. Note that we only consider the multi-cell MIMO RBF schemes. Discussions for the MISO RBF can be drawn from either the RBF-MMSE, RBF-MF, or RBF-AS by setting $N_R = 1$.

5.3.1. Single-cell case

First, we consider the single-cell case to draw some useful insights. It is well known that the maximum sum-rate DoF for a single-cell MIMO-BC with N_T transmit antennas and $K \geq N_T$ users each with N_R receive antennas under independent channels is N_T [1] [55], which is achievable by the DPC scheme or even simple linear precoding schemes. However, it is not immediately clear whether such a result still holds for the case of $K = \Theta(\rho^{\alpha}) \gg N_T$ with $\alpha > 0$, since in this case N_T may be only a lower bound on the maximum DoF. We thus have the following proposition.

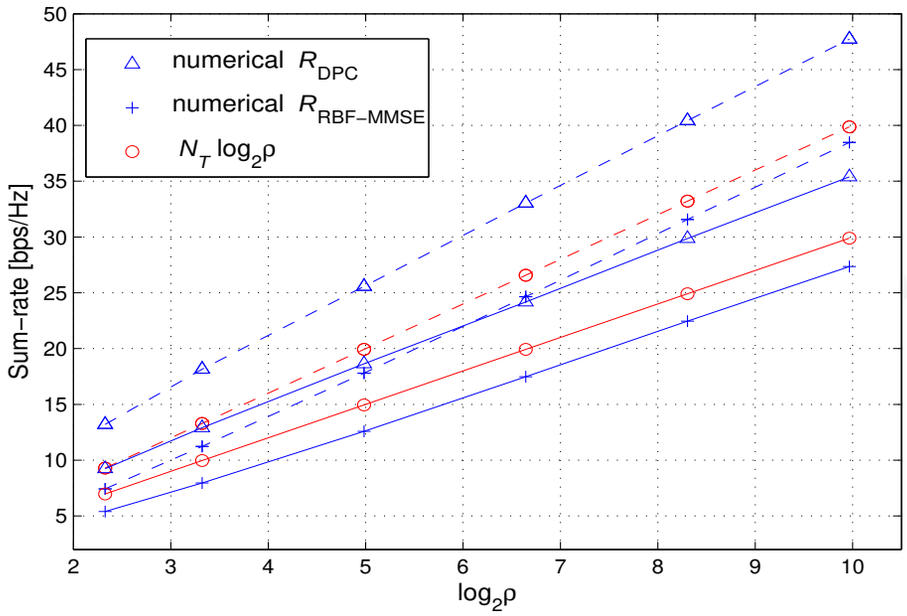


Figure 9. Comparison of the numerical DPC and RBF-MMSE sum-rates, and the DoF scaling law with $\alpha \geq N_T - N_R$.

Proposition 5.1. *([24, Proposition 4.1]) Assuming $K = \Theta(\rho^\alpha)$ with $\alpha > 0$, the maximum sum-rate DoF of a single-cell MIMO-BC with N_T transmit antennas is $d^*(\alpha) = N_T$.*

Proposition 5.1 confirms that the maximum DoF of the MIMO-BC is still N_T, even with the asymptotically large number of users that scales with SNR, i.e., multi-user diversity does not yield any increment of "interference-free" DoF. The optimality of the single-cell RBF schemes is given in the following proposition

Proposition 5.2. *([24, Proposition 4.4]) Assuming $K = \Theta(\rho^\alpha)$, the single-cell MIMO RBF-Rx scheme is DoF-optimal if*

- *RBF-MMSE: $\alpha \geq N_T - N_R$.*
- *RBF-MF/AS: $\alpha \geq N_T - 1$.*

From the above proposition, it follows that the single-cell MIMO RBF schemes achieve the maximum DoF with $M = N_T$ if the number of users is sufficiently large, thanks to the multi-user diversity effect that completely eliminates the intra-cell interference with a large number of users.

As an example, we compare the numerical sum-rates and the DoF scaling law in Fig. 9, in which the DPC and RBF-MMSE are employed, and $\alpha \geq N_T - N_R$. We consider two single-cell systems with the following parameters: (1) $M = N_T = 3$, $N_R = 2$, $\alpha = 1$, $K = \lfloor \rho^\alpha \rfloor$; and (2) $M = N_T = 4$, $N_R = 3$, $\alpha = 1.2$, $K = \lfloor \rho^\alpha \rfloor$. The rates and scaling law of system 1 and 2 are denoted as the solid and dash lines, respectively. Note that in both cases, the DPC and RBF-MMSE sum-rates follow the (same) DoF scaling law quite closely. This example clearly demonstrates the optimality of the RBF given a large per-cell number of users.

5.3.2. Multi-cell case

For the convenience of analysis, we use $\mathcal{D}_{\text{UB}}(\boldsymbol{\alpha})$ to denote an upper bound on the DoF region defined in (40), for a given $\boldsymbol{\alpha}$ in the multi-cell case. Clearly, under Assumption 1, it follows that $\mathcal{D}_{\text{RBF-Rx}}(\boldsymbol{\alpha}) \subseteq \mathcal{D}_{\text{MIMO}}(\boldsymbol{\alpha}) \subseteq \mathcal{D}_{\text{UB}}(\boldsymbol{\alpha})$.

The following proposition establishes the DoF region upper bound $\mathcal{D}_{\text{UB}}(\boldsymbol{\alpha})$.

Proposition 5.3. *([24, Proposition 4.3]) Given $K_c = \Theta(\rho^{\alpha_c})$, $c = 1, \cdots, C$, a DoF region upper bound for a C-cell downlink system is given by*

$$\mathcal{D}_{\text{UB}}(\boldsymbol{\alpha}) = \left\{ (d_1, d_2, \cdots d_C) \in \mathbb{R}_+^C : d_c \leq N_T, c = 1, \cdots, C \right\}. \tag{51}$$

The optimality of the multi-cell MIMO RBF-Rx schemes is shown in the following proposition

Proposition 5.4. *([24, Proposition 4.3]) Given $K_c = \Theta(\rho^{\alpha_c})$, $c = 1, \cdots, C$, the multi-cell MIMO RBF-Rx scheme achieves the "interference-free" DoF region of a C-cell downlink system, i.e., $\mathcal{D}_{RBF\text{-}Rx}(\boldsymbol{\alpha}) \equiv \mathcal{D}_{\text{UB}}(\boldsymbol{\alpha})$, if*

- *RBF-MMSE: $\alpha_c \geq CN_T - N_R$, $\forall c \in \{1, \cdots, C\}$.*
- *RBF-MF/AS: $\alpha_c \geq CN_T - 1$, $\forall c \in \{1, \cdots, C\}$.*

As a consequence, we also have $\mathcal{D}_{RBF\text{-}Rx}(\boldsymbol{\alpha}) \equiv \mathcal{D}_{MIMO}(\boldsymbol{\alpha})$, i.e., the RBF-Rx scheme is optimal given large per-cell user densities.

The above proposition implies that the multi-cell MIMO RBF schemes are indeed DoF-optimal when the numbers of users in all cells are sufficiently large. Due to the overwhelming multi-user diversity gain, RBF compensates the lack of full CSI at transmitters without any compromise of DoF degradation. However, it is important to point out that such a result should not undermine the benefits of having the more complete CSI at transmitters in practical multi-cell systems, where more sophisticated precoding schemes than RBF such as IA-based ones can be applied to achieve substantial throughput gains, especially when the numbers of per-cell users are not so large.

6. Summary

In this chapter, we have introduced the OBF/RBF and the current developments in the literature. First of all, we have given an overview for the single-cell case, summarizing some of the most important contributions so far. Furthermore, we have reviewed the recent investigations on the rate performance of multi-cell RBF systems in both finite- and high-SNR regimes. These results are useful for the optimal design of multi-cell RBF in practical cellular systems. In particular, it is revealed that collaboration among the BSs in assigning their respective numbers of data beams based on different per-cell user densities is essential to achieve the optimal throughput tradeoffs among different cells. Moreover, the results show that spatial receive diversity is also a significant factor to be considered, noting that there

exists, however, a tradeoff between the rate/DoF performance and the complexity/delay time of RBF systems with different receivers. The preference of multi-cell RBF is justified by the scheme's optimality albeit requiring only partial CSI at transmitters as compared to other full-CSI transmission schemes, when the numbers of users in all cells are sufficiently large.

Author details

Hieu Duy Nguyen, Rui Zhang, and Hon Tat Hui

* Address all correspondence to: nguyendh@i2r.a-star.edu.sg, elezhang@nus.edu.sg, elehht@nus.edu.sg

Department of Electrical and Computer Engineering, National University of Singapore, Singapore

References

[1] G Caire and S Shamai. On the achievalbe throughput of a multi-antenna Gaussian broadcast channel. *IEEE Trans. Inf. Theory,* 49:1691–1706, July 2003.

[2] M Costa. Writing on dirty paper. *IEEE Trans. Inf. Theory,* 29:439–441, May 1983.

[3] H Weingarten, Y Steinberg, and S Shamai. The capacity region of the Gaussian multiple-input multiple-output broadcast channel. *IEEE Trans. Inf. Theory,* 52:3936–3964, Sep. 2006.

[4] Q H Spencer, A L Swindlehurst, and M Haardt. Zero-forcing methods for downlink spatial multiplexing in multiuser MIMO channels. *IEEE Trans. Signal Process.*, 52:461–471, Feb. 2004.

[5] E Biglieri, A Constantinides, R Calderbank, A Goldsmith, A Paulraj, and V Poor. *Introduction to MIMO Wireless Communications*. Cambridge Univ. Press, June 2006.

[6] A B Gershman and N Sidiropoulos, editors. *Space-Time Processing for MIMO Communications*. John Wiley & Sons, 2005.

[7] A Paulraj, R Nabar, and D Gore. *Introduction to Space-Time Wireless Communications*. Cambridge Univ. Press, May 2003.

[8] A E Gamal and Y-H Kim. *Network Information Theory*. Cambridge University Press, 2011.

[9] S A Jafar. *Interference alignment: a new look at signal dimensions in a communication network*. Foundations and Trends in Communications and Information Theory, 2011.

[10] B Ng, J Evans, S Hanly, and D Aktas. Distributed downlink beamforming with cooperative base stations. *IEEE Trans. Inf. Theory,* 54:5491–5499, Dec. 2008.

[11] L Zhang, R Zhang, Y C Liang, Y Xin, and H V Poor. On the Gaussian MIMO BC-MAC duality with multiple transmit covariance constraints. *IEEE Trans. Inf. Theory,* 58:2064–2078, Apr. 2012.

[12] R Zhang. Cooperative multi-cell block diagonalization with per-base-station power constraints. *IEEE J. Sel. Areas Commun.,* 28:1435–1445, Dec. 2010.

[13] H Dahrouj and W Yu. Coordinated beamforming for the multicell multi-antenna wireless systems. *IEEE Trans. Wireless Commun.,* 9:1748–1795, May 2010.

[14] Y-F Liu, Y-H Dai, and Z-Q Luo. Coordinated beamforming for MISO interference channel: complexity analysis and efficient algorithms. *IEEE Trans. Signal Process.,* 59:1142–1157, Mar. 2011.

[15] E Bjornson, R Zakhour, D Gesbert, and B Ottersten. Cooperative multicell precoding: rate region characterization and distributed strategies with instantaneous and statistical CSI. *IEEE Trans. Signal Process.,* 58:4298–4310, Aug. 2010.

[16] X Shang, B Chen, and H V Poor. Multiuser MISO interference channels with single-user detection: optimality of beamforming and the achievable rate region. *IEEE Trans. Inf. Theory,* 57:4255–4273, July 2011.

[17] R Zhang and S Cui. Cooperative interference management with MISO beamforming. *IEEE Trans. Signal Process.,* 58:5450–5458, Oct. 2010.

[18] N Jindal. MIMO broadcast channels with finite-rate feedback. *IEEE Trans. Inf. Theory,* 52:5045–5060, Nov. 2006.

[19] P Viswanath, D N C Tse, and R Laroia. Opportunistic beamforming using dumb antennas. *IEEE Trans. Inf. Theory,,* 48:1277–1294, June 2002.

[20] M Sharif and B Hassibi. On the capacity of MIMO broadcast channel with partial side information. *IEEE Trans. Inf. Theory,* 51:506–522, Feb. 2005.

[21] M Sharif and B Hassibi. A comparison of time-sharing, beamforming, and DPC for MIMO broadcast channels with many users. *IEEE Trans. Commun.,* 55:11–15, Jan. 2007.

[22] H D Nguyen, R Zhang, and H T Hui. Multi-cell random beamforming: achievable rate and degree of freedom region. *submitted to IEEE Trans. Sig. Proc., available online at http://arxiv.org/abs/1205.5849*, 2012.

[23] A Tajer and X Wang. (n, K)-user interference channel: degrees of freedom. *IEEE Trans. Inf. Theory,* 58:5338–5353, Aug. 2012.

[24] H D Nguyen, R Zhang, and H T Hui. Effect of spatial receive diversity on the degree of freedom region of multi-cell random beamforming. *in preparation*, 2012.

[25] H-C Yang, P Lu, H-K Sung, and Y-C Ko. Exact sum-rate analysis of MIMO broadcast channels with random unitary beamforming. *IEEE Trans. Commun.,* 59:2982–2986, Nov. 2011.

[26] Y-C Ko, H-C Yang, S-S Eom, and M-S Alouini. Adaptive modulation with diversity combining based on output-threshold MRC. *IEEE Trans. Wireless Commun.,* 6:3728–3737, Oct. 2007.

[27] Y Kim, J Yang, and D K Kim. A closed form approximation of the sum-rate upper bound of random beamforming. *IEEE Commun. Lett.,* 12:365–367, May 2008.

[28] D Park and S Y Park. Performance analysis of multiuser diversity under transmit antenna correlation. *IEEE Trans. Commun.,* 56:666–674, Apr. 2008.

[29] H David and H Nagaraja. *Order Statistics*. New York: Wiley, 3rd edition, 2003.

[30] K Huang, J G Andrews, and R W Heath, Jr. Performance of orthogonal beamforming for SDMA with limited feedback. *IEEE Trans. Veh. Tech.,* 58:152–164, Jan. 2009.

[31] K Huang, R W Heath, and J G Andrews. Space division multiple access with a sum feedback rate constraint. *IEEE Trans. Veh. Tech.,* 58:3879–3891, Jul. 2007.

[32] L Sun and M R McKay. Eigen-based transceivers for the MIMO broadcast channel with semi-orthogonal user selection. *IEEE Trans. Sig. Proc.,* 58:5246–5261, Oct. 2010.

[33] J L Vicario, R Bosisio, C Anton-Haro, and U Spagnolini. Beam selection strategies for orthogonal random beamforming in sparse networks. *IEEE Trans. Wireless Commun.,* 7:3385–3396, Sep. 2008.

[34] T Yoo and A Goldsmith. On the optimality of multi-antenna broadcast scheduling using zero-forcing beamforming. *IEEE J. Sel. Areas Commun.,* 24:528–541, Mar. 2006.

[35] R Couillet, J Hoydis, and M Debbah. Random beamforming over quasi-static and fading channels: a deterministic equivalent approach. *to appear in IEEE Trans. Inf. Theory, available online at http://arxiv.org/abs/1011.3717*, 2012.

[36] O Ozdemir and M Torlak. Optimum feedback quantization for an opportunistic beamforming scheme. *IEEE Trans. Wireless Commun.,* 9:1584–1593, May 2010.

[37] S Sanayei and A Nosratinia. Opportunistic beamforming with limited feedback. *IEEE Trans. Wireless Commun.,* 6:2765–2770, Aug. 2007.

[38] Y Xue and T Kaiser. Exploiting multiuser diversity with imperfect one-bit channel state feedback. *IEEE Trans. Veh. Tech.,* 56:183–193, May 2007.

[39] J So and J M Cioffi. Feedback reduction scheme for downlink multi-user diversity. *IEEE Trans. Wireless Commun.,* 8:668–672, Feb. 2009.

[40] A Rajanna and N Jindal. Multi-user diversity in downlink channels: when does the feedback cost outweigh the spectral efficiency benefit. *IEEE Trans. Wireless Commun.,* 11:408–418, Jan. 2012.

[41] A Barg and D Yu Nogin. Bounds on packings of spheres in the Grassmann manifold. *IEEE Trans. Inf. Theory,* 48:2450–2454, Sep. 2002.

[42] B M Hochwald, T L Marzetta, T J Richardson, W Sweldens, and R Urbanke. Systematic design of unitary space-time constellations. *IEEE Trans. Inf. Theory,* 46:1962–1973, Sep. 2000.

[43] D J Love and R W Heath. Grassmannian beamforming for multiple-input multiple-ouput wireless systems. *IEEE Trans. Inf. Theory,* 49:2735–2747, Oct. 2003.

[44] N Zorba and A I Perez-Neira. Opportunistic Grassmannian beamforming for multi-user and multi-antenna downlink communications. *IEEE Trans. Wireless Commun.,* 7:1174–1178, Apr. 2008.

[45] M Xia, Y-C Wu, and S Aissa. Non-orthogonal opportunistic beamforming: performance analysis and implementation. *IEEE Trans. Wireless Commun.,* 11:1424–1433, Apr. 2012.

[46] M Kountouris, D Gesbert, and T Salzer. Enhanced multiuser random beamforming: dealing with the not-so-large number of users case. *IEEE Trans. Wireless Commun.,* 26:1536–1545, Oct. 2008.

[47] H Kwon, E W Jang, and J M Cioffi. Predetermined power allocation for opportunistic beamforming with limited feedback. *IEEE Trans. Wireless Commun.,* 10:84–90, Jan. 2011.

[48] J Wagner, Y C Liang, and R Zhang. On the balance of multiuser diversity and spatial multiplexing gain in random beamforming. *IEEE Trans. Wireless Commun.,* 7:2512–2525, July 2008.

[49] I H Kim, S Y Park, D J Love, and S J Kim. Improved multi-user MIMO unitary precoding using partial channel state information and insights from the Reimannian manifold. *IEEE Trans. Wireless Commun.,* 8:4014–4022, Aug. 2009.

[50] H Kushner and P A Whiting. Convergence of proportional-fair sharing algorithms under general conditions. *IEEE Trans. Wireless Commun.,* 3:1250–1259, July 2004.

[51] H Zhou, P Fan, and J Li. Global proportional fair scheduling for networks with multiple base stations. *IEEE Trans. Veh. Tech.,* 60:1867–1879, May 2011.

[52] I S Gradshteyn and I M Ryzhik. *Table of Integrals, Series and Products*. Jeffrey, A. & Zwillinger, D. (eds), Academic Press, 7th edition, 2007.

[53] S-H Moon, S-R Lee, and I Lee. Sum-rate capacity of random beamforming for multi-antenna broadcast channels with other cell interference. *IEEE Trans. Wireless Commun.,* 10:2440–2444, Aug. 2011.

[54] H Gao and P J Smith. Exact SINR calculations for optimum linear combining in wireless systems. *Prob. Eng. Inf. Sci.,* 40:261–281, May 1998.

[55] Y Huang and B D Rao. Closed form sum-rate of random beamforming. *IEEE Commun. Lett.*, 16: 630-633, May 2012.

IntechOpen

IntechOpen